ACP review:

This is a point to point response to the **Ref#1** comments.

Referee comments are in italic.

We would like to thank the referee for his/her numerous comments, suggestions and technical corrections that made the paper so much better. We really appreciate the enormous amount of time you spent with our manuscript.

P1L31: Please specify "and other global datasets"

- *P1L38: Specify "changes of the middle atmosphere"*
- *P2L25: What other phenomena cause abrupt changes of MA circulation? If not relevant, please rephrase.*
- *P2L32: Explain here (shortly) again why. Mention again PW generation by IGW if relevant.*
- *P2L39: processes such as e.g. ...? List shortly.*

Answer: The introduction underwent minor changes based on you and Ref#3 comments.

P4L2: What do you mean with "introduce"? Do you mean prescribe? Nudge?

"prescribe" is the right word, it is changed (P3L29)

P4L8: How long is the spin-up period?

330 model days, has been added in the text (P3L36)

P4L10: Mean January conditions? Of what period? Or a specific January? In this context, take into account the comments of referee #3

Decadal mean January means are used and this is now mentioned in the text (P4L9).

P4L25-26: Can this abrupt change lead to dynamic instabilities during the transition?

Answer: Yes. The build up of the response is to see in Hovm. diagrams (Figs. 3, 4 and 9).

P4L22-28: Should this GWD modification be understood as rather a change in orographic or non-orographic GWs or as a mixture? Can you estimate that from the observations in Sacha et al. 2015?

Answer: Based on Šácha et al. 2015 and on analysis of CMAM-sd GW parametrization output (not shown) we argue that the majority of GWs in the stratosphere in the EA/NP region in January are of orographic origin (P5L24).

P4L37: Please explain why you are not smoothing the boundaries and if that could have any effect.

Answer: To simulate the sudden and localized GW breaking effect and also to mimic the EA/NP hotspot given the coarse resolution of the model. It is very likely that the sharp boundaries will determine some patterns of the response (e.g. the lee wave pattern in Fig. 10b)-P16L2-4. In the Box0.1 simulation the boundaries are not as sharp due to the background GWD from the reference simulation.

Table 1: Please explain better the systematic behind these experiments. Many values of the table cannot be found in the text. Are these values random guessing (trial and error) or is there a particular science question behind every combination of values?
Answer: We are describing the choices of the GWD components P5L12-30. To summ up, we are varying the GWD along the rough observational constraints (or estimates) for the GWD above the EA/NP region.

Sect. 2.2: It should be made a lot clearer in this section what can be compared here. The model does not seem to calculate interactive chemistry for ozone and methane, and these tracer distributions do not reflect purely dynamical effects (which is mentioned). At this point I do not see how 30 day model simulations (with only January conditions) are supposed to be compared with 30 year annual climatologies of satellite observations. Moreover, are these satellite observations in well enough resolution (temporal and spatial) to hold for comparisons with the effects studied in the model?
Answer: The comparison has been removed and the tracer related information is now given in the supplement only for motivation of research in the EA/NP region.

P6L6: Explain why you analyse the 6.25hPa level.
Answer: It is the second level above the artificial GWD and nudging upper boundary. The first level above can be influenced by some interface effects. We have added a clarification of this choice at P6L15-18.

P6L13: The SSW simulations have not been explained before (only in the table). There should be information in the main text about those.
P6L21-33: This paragraph should be revised comprehensively. Fig. 2 should be split into two or three figures, in the print-out version, the wind vectors are hardly visible and also the other features are not clear. The meaning of the mentioned results are not clear (particularly line 24-26) and the sentence from line 27-30 should be split to make the points one by one. Also, the word "quite" in line 28 should be removed or specified.
P7L26-28: This mechanism should be explained better and/or citations included.
P7L30-32: This should be in the discussion and outlook section, maybe the entire paragraph.
Answer: The SSW simulations are now introduced in Fig.4 and related discussion. Wind vectors in Fig. 5 (former Fig.2) have been enlarged and the subsection related to Fig. 5 has been rewritten.

P8L5: over how much time is that strengthening and shift taking place?
P8L11-12: This statement should be constrained further in such way that the robustness of this behaviour has not been tested in other vortex situations.
P8L15: How can I see that this vortex displacement is more rapid?
Answer: Fig. 4 has been added to give additional information about SSWs and the description of results is now more precise and clear P8L24-P9L12.

In general: At many places, line breaks should be used instead of blank lines everywhere. This would help to divide the respective sections into individual units of meaning.
Answer: We are using the ACP template where blank lines seem to be the only way to divide paragraphs. But we agree that this would be helpfull.

Fig 4: You do not discuss Fig. 4d in the text here, instead you mention one "not shown" figure and one figure from the Supplement. You should consider to restructure this. Also, I would appreciate the contoured lines for the box of enhanced GW drag, as in 4f, in all panels. However, why are there 3 lines, is it not always the same box?
Answer: Fig. 7 (former Fig.4) as well as other figures has been newly created and the choice of subplots now fits better to the direction of the text.

P10L12: This (rather abstract) figure should be introduced with some motivation why you plot this and/or what you expect to learn from plotting this.
Answer: The motivation for Fig. 9 is at P11L15-18 and its results are newly described.

P12L18: What else can it be? And what does that mean for the simulations?
Answer: After the comment from Ref#3 we have made a much deeper analysis with the outcome that this pattern is most likely caused by nonlinear interaction of inertia GWs with tides (P12L5).

P13L13-21: This comparison does not seem sensible to me. CH4 is influenced by much more than only vertical velocity (chemistry, advection, diffusion) and thus the comparison does not hold. Also, the patterns you describe in the plots are hardly visible and the motivation for this comparison is not clear to me either. I am not sure if the comparison is crucial for your results anyway, since you do not conclude any vital points here, but if so, the comparison should be made much more carefully.
Answer: This subsection has been deleted.

Section 4: I think this section should be revised comprehensively. Now, it is some mishmash of discussion, outlook (partly irrelevant like P16L36), conclusions and literature review (partly with only little relation to the results of this study, e.g. P17L8-12). It should be structured more thoroughly around the results of this study and link the findings more clearly to the literature (e.g. P15L26-32: It feels like there lacks a (half) sentence at the end that integrates your results into the ones from the references mentioned). The second paragraph is a literature re- view without any clear connection to the results, rather, it raises questions that cannot be answered with this setup; that seems out of place. The second para- graph discusses some insufficiancies of the idealistic modelling approach. This is indeed very important, but it is not made clear, what that means for the con- clusions that can be drawn from the model experiments (what can/could still be learned out of the vortex displacement simulation even though it is not reliable?). The connection of your results with the PDO should be discussed more thoroughly because from your model setup (mean January) you cannot compare different PDO phases. Moreover, the PDO had never been mentioned before in the paper.

There should be a separate and concise conclusions section that lists the main findings of this study (one of which e.g. an extract of the last paragraph of the paper, this is a very important point).

Answer: We absolutely agree and the Discussion and conclusions section has been restructured, rewritten and a summary of results is now given at P14L30-P15L24.

All of the following technical corrections have been implemented and the animations are now created according to ACP guidelines.

ACP review:

This is a point to point response to the **Ref#2** comments.

Referee comments are in italic.

We would like to thank the referee for his detailed insight into the intermittency of GWs and the relevance of our GWD enhancement.

I support the comment of Referee#3 that for fully appreciating the results, it is necessary to assess the variability of the model and the influence of this on the results.

Answer: The variability of the model is now better described and all of the mean plots now come with an estimate of statistical significance. Please see the response to Ref#3.

Both the authors and Referee#3 emphasize the intermittency of gravity waves. The quoted intermittency investigations focus on the high variability considering single waves / individual observations. This intermittency may be used for instance to de- velop / improve GW parametrization schemes (de la Camera et al., JGR, 2014). The situation is different, however, if we consider regional averages. Regional averages for regions with prominent mountain wave forcing also yield highly intermittent GW vari- ances and GWMF, with variations of more than an order of magnitude from day to day (e.g. Eckermann and Preusse, 1999, Jiang et al., JGR, 2002, Schroeder et al., GRL, 2009). The situation is different, for instance, for subtropical convective gravity waves (i.e. summer subtropics). Considering single wave events, there is also large intermittency between events. GWMF and also other wave parameters (phase speed, wavelengths) are highly variable. Considering a larger region as in the current paper, the average behavior however does vary much less (e.g. Schroeder et al., GRL, 2009). For the wintertime forcing discussed here, shear would be a likely source (e.g. Leena et al., JASTP, 2012; Pramitha et al., ACP, 2015; Atmos. Res. 2016). Unfortunately, we have for this forcing a lack of sufficiently frequent remote sensing observations (i.e. in- sufficient temporal resolution), in order to quantify the temporal variability, but it may be argued that also the winter time regional average would not lead to strong pulses (i.e. day-to-day variations). Thus, assuming a constant forcing after the onset of some gen- eral meteorological condition, seems a plausible assumption and therefore focussing on the average response after a few days a plausible approach.

Answer: Based on your comment we are discussing this at P15L33-35 and the reference Schroeder et al., 2009 is added.

ACP review:

This is a point to point response to the **Ref#3** comments.

Referee comments are in italic.

At first, we would like to thank the referee for all of his comments, ideas and suggestions. The manuscript has been greatly improved thanks to the time he devoted to our manuscript.

Major Concerns:

1) The results of the paper are based on a number of 30 day simulations with the MUA (Middle and Upper Atmosphere) Model. In the real atmosphere, there is substantial natural variability, and results based on a single 30 day snap shot would likely be meaningless in a statistical sense. I suspect that this model does not have much natural variability – otherwise the authors would not be able to conclude much from such short runs – but that is unclear in the current paper, which provides little insight into the background flow and no discussion of the statistics.

To remedy this situation, I recommend first establishing the quality of the model, better characterizing its January climatology (for example, showing the zonal mean wind as a function of pressure and height) along with the variability (for example, the variance of the zonal mean winds). Does this model vary much at all, or it essential steady, seeking only to capture the climatological mean circulation. It would also be good to show the overall impact of the gravity wave drag (GWD) scheme. A panel/overlay showing the zonal mean drag as a function of pressure and latitude might help, too, giving us a better sense the background gravity wave driving.

Answer: We absolutely agree and therefore we made major changes in the manuscript:

In section 2.1, the model, its variability and the procedure of creation of the sensitivity simulations are desribed in more detail. Information about the reference simulation is given in Fig.1. In Figure 3 and at the start of the Results section we now establish the time scale of the response and statistics is now included everywhere in the manuscript, where mean anomalies or differences are dealt with. Standard deviations of the zonal means in the reference simulation in the 30 days are small as described in the text (P4L10-15).

Then, how sensitive are these quantities to the forcing? At the top of page 4 the authors suggest they force planetary waves 1, 2, and 3 from ERA-I reanalysis at 1000 hPa. Do they mean climatological waves (based on what period)? What would happen if you took the waves from a given year? My concern here is that the authors need to estab- lish that their results are robust, and wouldn't change dramatically if the climatology is altered. Varying the lower boundary would allow them to sample the natural variability of the real world; in his case they would need need to run a number of simulations for each case, and could assess the statistical robustness of their conclusions.

Answer: The waves are extracted from decadal mean ERAI reanalysis and are stationary only (P3L35). The words "decadal monthly mean" have been included

(P3L30) to point that out. The model reaches a steady state after the spin-up (Fig. 3A).
More general answer from the AC1:
We agree with this comment. The overall response will be different for different background conditions. But there is a question, how reasonable it is to compare the responses of different background states to the same GWD. Naturally, each different background state means different GW sourcing and propagation conditions that should result to a different GWD. With our artificial enhancement approach we are not able to reflect this. Instead, in our simulations we have chosen a different approach. For mean January conditions we inject GWD settings stemming from our estimation based on observations (and from uncertainties especially in its meridional component) and from the mean climatology in the EA/NP region. In our paper we wanted to shed the light on the acting mechanisms and patterns of local response (e.g. build up of a positive geopotential anomaly upstream from the GWD, obstacle analogy..) that we assume will remain valid also for sligthly different conditions.
Actually, we have also made simulations with slightly different background climatology and the results were almost similar (absolute agreement in the pattern, only the magnitude was slightly different in some places). We would not like to show the figures in the revised manuscript, because we think that it would have little additional value, since in our manuscript we are not exactly concerned with the precise magnitude of the response.

And finally, all figures need to acknowledge the statistics. I don't mean to be the curmudgeon who rants that a result without an error bound isn't a scientific result, but you do need to either estimate the statistical certainty, or explain that everything that is shown is robust, given the lack of variability in the model.

Answer:We absolutely agree and thank the referee for pointing out this. In a revised manuscript all of the mean (from day 7 to 30) differences and anomalies are overlaid with stippled areas of significance exceeding the 5% level (p- value estimated using the t-test). Except the new Fig. 9, where the standard deviation is dotted.

2) Following up on my first concern, it is unclear to me what these experiments are seeking to represent. Many figures (e.g. 2, 4, etc.) show the 30 day mean, which initially suggested to me that the goal was to demonstrate the steady response to the wave driving (which I presumed had occured over this time scale). But it was not until the Fig. 5 that I realized that the response had clearly not converged over this period!
Gravity waves in the real world tend to be episodic and highly itermittent, so that the short term response is highly relevant. But if the goal is to capture the short term response, then I think the paper needs to focus on this from the start, and establish the appropriate time scale early on. This could be done, for example, by showing a Hovmoller diagram of some key quantities, such as the zonal mean wind at 6 hPa (or another key level) as a function of latitude and time, along with the evolution of the evolution of the key zonal harmonics (as in Fig. 5), but again, plotted as a function of latitude and time. The goal would be to show that the key change(s) occur on a timescale of X days (where X is with hope < 30 days!),

establishing that a short 30 day run is sufficient for the study. And then subsequent figures could focus on the key time period(s). I say periods because Fig. 5 hints that there is some oscillitory nature to the response.

Answer: The paper has been significantly improved in terms of structure, clarity and description of results. We now also make it absolutely clear what our simulations seek to represent (P6L30-38) - mean response to a monthly mean GWD distribution (as is usual from satellite observations). Following the comments made by the referee, we use Hovmöller diagrams to establish the time interval, which can be considered as quasi-steady (from ca 7 days to the end of simulation, see Fig. 3). This allows us to compute mean responses, but only for simulations with -0.5 and -10 m/s/day artificial GW induced zonal acceleration. For -70 m/s/day the simulations do not reach a steady state during the simulation. The responses in those "SSW simulations" are always presented as snapshots in selected time steps (Figs. 6, 8) or as animations (Animation 1a, b, 2 and 4). In the revised version, in addition, we present time evolution of zonal mean zonal wind to prove the SSW like nature of the vortex events (Fig. 4).

I still worry, however, that the short term response may depend a lot on the initial condition as discussed above. For example, in the real world, the propagation and breaking of gravity waves will be very different if the polar vortex is very strong vs. very weak (i.e. after a Sudden Warming). So one ideally would want to sample over different background states to robustly establish the short term response. [I assume the authors are forcing the model with some climatological mean wave forcing, but would it make a difference to use waves from a given year, etc.?]

Answer from the AC1: This is true, but the problem is that our GWD injection (value and ratio) is constant, not taking into account the background. With a little exaggeration we can say that for each time step in each ensemble member we would need another GWD enhancement values and only then we can sample for a robust response. We think that the presented results stemming from injection of constant GWD (estimated in accordance with the mean background conditions) are good enough to analyze the nature of the response as well as the discrepancy between effects of localized and zonally symmetric forcing.

I do appreciate that the authors have provided information about the time evolution in supplementary videos, but I feel that the time evolution is vital to the paper, and can't be left in the supplement.

Thanks to the referee's suggestion we use Hovmöller plots where the information on time evolution was important (Fig. 3, 4, 10). The animations in the supplement are now rather for interested readers. The paper is consistent without them and the volume of text discussing them has been minimalized. But we strongly encourage everyone to take a look at the animations, since some features are much more clear from the animation.

*3) I think it would help the paper to organize around key scientific question(s) and results. The discussion/conclusion section was more a discussion of other papers, and left me a bit confused as to what *this* paper was trying to say. In it's current* *form, the paper comes across as a bit descriptive, e.g. we tried this, and this happened. I appreciate that this is how science often moves forward, but in the conclusions, I urge them to step back and summarize how these simulations do give us new understanding.*

Answer: The organization of the paper has not been changed. This means division into polar vortex, PW and residual circulation response sections. But thanks to the comments from all referees, the entire Results section has been improved. Discussion section has been restructured to be more focused and the summary of results is given P14L28-P15L24.

I really think there is a lot of potential material here, just that the authors need to better focus the paper. Here are two key areas that could be the main result – just one or would be sufficient – and I don't mean to restrict the authors to these points.
*(a) Based on my own interests, I was particularly excited about the zonal mean response to zonally asymmetric wave driving. Given that downward control indicates that the time mean residual circulation depends only on the zonal mean wave driving, one might think that the zonal structure of the gravity wave driving should not matter. But since zonally asymmetric GWD induces a response in resolved waves, the *total* zonal mean wave driving depends very much on the zonal structure of the GWD. To show this, downward control analysis and more discussion of the compensation and interaction between resolved and parameterized wave driving would help.*
The authors acknolwedge that nudging might limit the zonal mean response, and so drive compensation by itself. Initially I though the nudging was done to "improve the troposphere", but upon re-reading, I realized it extends to 30 km, fairly deep into the stratosphere! How strong is the nudging in the stratosphere?
Can you estimate it's effective amplitude, and compare it to that of the applied gravity wave driving? Down- ward control can still be applied, but you just need to account for the torque produced by the nudging.

Answer: For a detailed response to the first paragraph, please see the AC1 - In short, this is a highly interesting topic and we want to perform such an analysis in near future.
Regarding the nudging, it is dependent on the strength of the zonal mean response. It acts on zonal mean temperatures in MUAM and the magnitude ranges from lesser than 1K/day for the reference simulation to almost 2K/day for the SSWbox simulation (See Fig. 1c in the revised manuscript). An explanation of the role of nudging in MUAM (P3L37-P4L5) and a figure of the strength of nudging for the SSWbox have been added (Fig. 1c). To minimalize the effect on our results we analyze (except Figs. 7 and 8, 11 and 12) our results two layers above the nudging upper boundary.

(b) Another important and novel key result could be the impact of localized GWD on he overall resolved wave structure, following up on the Holton (1984) result that asymmetric GWD generates planetary waves. In this case, I think the time evolution of the flow is much more important. The key would be to establish how fast the resolved flow responds to the gravity wave driving, the dependence on the

background state, the linearity of the response, and so forth. These results are in the paper, but I just feel they get lost in the discussion at the end.
Note that result (a) is more about the steady/climatological response, while (b) would be more about the time evolution. Once you know the targeted result, earlier figures could help lead the way.

Answer: In the revised manuscript the section 3.2 has been rewritten to focus more on the PW generation by GWD. Also, time evolution is taken into account (new Fig. 10). But as stated in AC1, a detailed analysis of the dependence on a background state is impossible with the concept of artificial injection we are using.

4)Overall, the presentation of the paper needs to be improved. Small things, such as keeping the names of the simulations uniform and avoid non-standard acronyms (e.g. "gcu, gcv, gt"), and keeping the orientation of the latitudinal axes constant, really do help the reader. I appreciate that the first author is a student, and when I look back at my first papers, I'm embarrassed by the barely perceptible contour lines and tiny font size of the figures. So please take the comments below as suggestions on how the presention could be improved, not as an attempt to be overly critical.
And as will come out in the detailed comments below, I think the paper relies to much on supplementary material. In my opinion, it's okay to have additional figures/movies for the curious reader, but all the key results of the paper should be within the paper.

Answer: The text in all sections underwent major revisions. The names of simulations were uniform already in the previous version - according the naming convention (except the SSW and specific simulations that are better characterized by shorter names): "*gcu + distribution + gcv + sign of gcv*", where gcu = -0.5 m/s/day is not stated in the name. This is now made clear at P4L35.
The acronyms are unchanged *("gcu, gcv, gt")* and are properly defined in the text (P4L26-27), because we are not aware about any standard acronym for those GWD components.

Other suggestions by page:line number:

1:28-34 This first sentence about Holton 1983 is a bit confusing/vague, and then there is a giant leap of 30 years to the present.
Answer: Deleted.

1:39 Perhaps you could say "ozone and greenhouse gases" instead of "climate change gases". Also, the references here are for the mesosphere and thermosphere, but not the stratosphere. For the stratosphere, observed temperature trends have been a bit more puzzling, e.g. Thompson et al. 2012, Nature.
Answer: Deleted.

More generally, how does the second paragraph on climate change relate to the results of this paper? If you really want to cover all of climate change in the middle atmosphere, and how well models appear to simulate it, you would need a lot more

references. But I this would be taking the paper off track. It might be sufficient to shorten this paragraph and direct the reader to review papers that highlight the significance of the stratosphere (e.g. Kidston et al. Gerber et al.,) and recent analyses of the CMIP5 models, (e.g. Charlton et al. 2013 and Manzini et al. 2014), which assess the "state of the art" when it comes to modeling. I think the goal should be to quickly get across the message that the stratosphere matters, and then zero in on your topic.
Answer: The paragraph has been shortened and the reference Manzini et al. 2014, added. P1L34

2:10 "The BDC is still..."
More generally, it's my understanding that this paragraph is trying to highlight the fact that the "BDC" is a slippery creature to define. It was first discovered based on the distribution of trace gases by Brewer (1949) and Dobson (1956). It is often quanti- fied by the residual circulation (Dunkerton 1978), which can be closely linked with the isentropic circulation. But tracers with geographically varying sources/sinks (such as ozone) are also transported by Rossby waves along isentropic surfaces, a process re- ferred to as isentropic mixing. To understand the movement of water vapor or ozone, you need to account both for the residual mean transport and the isentropic mixing. Plumb (2002) is a good paper to highlight this. However, you can still make a lot of progress with tracer distributions in a 2D context, based on the interplay between the residual circulation and mixing. The three dimensional structure is a new frontier in re- search, seeking to explain the detailed 3-D structure of temperature and trace gases.
Answer:The paragraph about BDC has been rewritten based on the referee comments (P1L38-P2L7).

2:22 I would say that the discussion on pre-conditioning is still an active area of re- search, though "agreement" is building.
Answer: The text was changed to (P2L11-12): There is a building agreement in the literature on the role of wave activity in preconditioning sudden stratospheric warming

page 3 general comment.
There have been a few other studies that have considered the impact of localize wave torques, and they would be relevant to your discussion.
Shaw, T. A., and W. R. Boos, 2012: The tropospheric response to tropical and subtrop- ical zonally-asymmetric torques: Analytical and idealized numerical model results. J. Atmos. Sci., 69, 214-234.
Naftali Y. Cohen, and William R. Boos, 2016: Modulation of subtropical strato- spheric waves by equatorial rainfall, Geophysical Research Letters, 43, 466–471, doi: 10.1002/2015GL067028
In addition, this paper follows up on Cohen et al. 2013 to discuss the mechanism behind compensation in greater detail. I mention it because it discusses the time scale of the response to forcing. In the stratospheric surf zone, they find it's very quick, reaching near equiliberium 5-10 days.
Naftali Y. Cohen, Edwin P. Gerber and Oliver Bühler, 2014: What drives the Brewer- Dobson circulation? Journal of the Atmospheric sciences, 71, 3837–3855, doi: 10.1175/JAS-D-14-0021.1

Answer: Thank you for bringing those papers into our attention. Studies Shaw and Boos (2014)-P14L10- and Cohen et al. (2014) -P3L4, P6L37, P9L37, P16L7.

First paragraph on 2.1. It might help the reader to explain a bit more about MUAM here. I gather that the model includes a troposphere, as the bottom is 1000 hPa, but is the troposphere very unrealistic, given the fairly coarse resolution? Does is it have an active tropospheric circulation with synoptic variability, or is the troposphere passive, and simply there to communicate the surface planetary wave forcing up to the tropopause? Explaining a bit more detail about the nudging might be appropriate here, too. How strong is it above the tropopause?
For context, there are models that just capture the middle atmosphere, e.g. Scott and Polvani (2006), where the lower boundary condition is the geopotential height near the tropopause? Here, the lower boundary to the stratosphere is completely specified, but it was clear to me how it works in MUAM. 4:6-8 To explain my confusion above, this sentence suggest that "PW and tides" are added. Perhaps the authors mean, "develop", as they are internally generated, right? They are not specified exactly, as implied by "added". [My apologies if this is just a linguistic issue.]
4:7 Does the model spin up to a steady state? Or is it chaotic (like the real atmosphere), that it spins up eddies, etc.. and the initial condition does matter.
4:13 It might be more helpful to report the source stress than the velocity amplitude.

Answer: As we only use monthly mean reanalysis data the troposphere is not meant to be a representation of a synoptical state but rather a monthly mean climatology. This has been pointed out, now (P3L30). Furthermore, we included a sentence making clear why the troposphere is necessary and why it needs to be corrected (P3L33).The word “added” is replaced by “generated”(P4L7). An additional figure with zonal mean winds, temperature and GWD has been included (Fig. 1), standard deviations of the zonal mean within these 30 days are small as described in the text (P4L10-P4L15). Nudging is described at P3L37-P4L5.

4:35 Even though the parameters do not change, I believe that the drag can change in response to changes in the resolved flow. It might be good to emphasize this, especially if these changes are not trivial.
Answer: We agree that it should be like this, but it is not the case in our simulations, as stated at P5L4-5. In our sensitivity simulations the GW parameterization scheme is switched off and we use the GW parameterization output from the reference simulation.

4:36 Cohen et al. 2013 suggest that sharp changes in gravity wave forcing are highly likely to be compensated, as the resulting circulation wouldn’t be stable otherwise.
Answer: This is now referenced at P5L9-11.

5:4 By "not covered by ... the reference run" do the authors simply mean that there is no enhanced gravity wave drag in these longitudes in the reference parameters.

Answer: The sentence has been rewritten to: There are no exceptional GWD values in the reference simulation in this region. P4L39.

5:5-12 Alexander and Rosenlof 1996 make some useful estimates of the "missing" drag that is likely explained by gravity waves. At 10 hPa, the estimate values around -1 m/s. (In general, I think we do know that net effect of gravity waves, at least in the lower stratosphere, is to decelerate the flow. Palmer et al. 1986, a pioneering study on gravity wave parameterization, added gravity waves to slow down the flow. I was therefore a bit surprised that net effect of gravity waves in Fig. 1 was generally a positive acceleration in the winter hemisphere. What level is shown here?

Answer: In Fig.2 (old Fig.1), GWD is plotted at approximately 14hPa (11th model level). We must confess that, at the start of our analysis, we were not satisfied with the performance of the MUAM GW parameterization output in the stratosphere and therefore we have chosen to modify it artificially.

Section 2.1 general comment: I may have missed it, but it was hard for me to find the vertical structure of the enhanced gravity wave drag. The horizontal structure is detailed at 4:29, but where do you explain the vertical structure? I assume the net acceleration is constant in height?

Answer: The vertical structure is now illustrated in Figs. 7,8, 11 and 12. The artificially added GWD is constant with height, but the total GW acceleration is not constant with height, because the artificial GWD is added to the reference field (very small background value). We included zonal mean latitude-height plots for GWD components from the reference simulation in Fig. 1d, e and f.

5:30-38 This is what I was trying to get out in my comment on page 2 and the BDC. It is not trivial to match the residual circulation, or even the three dimensional residual circulation, to tracer distributions because mixing plays a large role in their transport.

Answer: We deleted the part relating the residual circulation to the tracer distributions. Plots of tracer distributions are now given in the Supplement only (Fig. 1S, 2S) to give a motivation for research in the EA/NP region.

Table 1 I strongly recommend a uniform naming convention for your simulations. Why switch from Box0.1 to Box0.5 to 10Box to SSWBox. The last simulations should be Box10 and Box70 for consistency.

Also, what is "pos" in Box0.1pos supposed to indicate? I guess you mean than additional positive (northerly) wave drag has been added, but it's not clear why this makes it "pos".

Answer: We think that the names of simulations were uniform already in the previous version - according the naming convention (except for the SSW simulation and other specific simulations that are better characterized by shorter names): "*gcu + distribution + gcv + sign of gcv*", where gcu = -0.5 m/s/day is not stated in the name. This is now made clear at P4L35.

6:13 I don't really understand why you call this an SSW. It is true that putting a massive wave drag into the stratosphere kills the vortex, but is this really an SSW? Is it sudden, or does the vortex simply decelerate in response to the massive drag?

Answer: We have added Hovmöller diagrams to illustrate the time evolution of those observed vortex events (Fig. 4). Of course, the dynamics is visible most easily from Animation 1a and 1b in the supplement.

6:20-23 I do not understand this sentence.
6:23-24 before discussion positive/negative interference, it might be good to establish that these anomalies are indeed linear.
General comment on Figure 2: I found this figure hard to interpret. It might help to break it down a bit (or at least discuss it more slowly), to first help the reader understand the basic response of the model, and then it's sensitivity to different features.
It would help a lot to include titles above each plot, as I was constantly going up and down from the caption trying to understand what I was looking at. And the contour interval / color scale is changing all over the place. It's okay to use different color scale for the total field vs. anomaly fields, but otherwise, please fix them, so one can more easily compare panels.
Answer: The description of results shown in Fig. 5 (former Fig. 2) has been significantly improved and clarified. In Fig. 5, titles are now included.

6:33-7:4 It might be good to refocus the figure on these key results that you want to show.
It seems rather intuitive to me that the local (zonally asymmetric) response to Box gravity wave should be larger than the zonal gravity wave: the local amplitude is much larger when you focus it on a narrow region. Is the zonal mean response that much different? This seems to be a more relevant (and potentially interesting) question. As the zonal mean forcing is the same in both cases, should we expect the zonal mean response to be the same?
Answer: Titles in Fig. 5 now inlude also the sum of the geopotential response over the whole domain showing that the zonal mean response is indeed that different.

7:2-4 This discussion on nudging was a bit disconcerting. That's why I recommend explaining it in more detail to the reader earlier (as noted above).
Does the nudging imply that the zonal uniform response to the gravity wave drag is largely constrained, such that my questions above the zonal mean response above can't really be asked with this model?
Answer: In Fig. 1c and in the text at P3L37-P4L4 we are discussing the effect of nudging and its possible role. It acts to lower the zonal mean response, but it is not to that degree to affect the results of our analysis.

7:5-18 This discussion was confusing for me. Are the authors comparing the response to their gravity wave perturbation at 6.25 hPa with the response in to greenhouse gas forcing at 850 hPa in He at al. 2015? If so, this makes little sense. I suggest removing this paragraph entirely, or explaining why this comparison is relevant.
7:17-18 Why would you expect this? And again, how can you compare the response of the mid stratosphere to the near surface?
Answer: This paragraph has been removed.

More generally, is the response linear; i.e. if you increase the forcing by a factor of 10, does the response scale up by a factor of 10? This would be a good thing to establish.
Answer: Phrases implying the need of linearity were rephrased in the text and two sentences have been added (P8L14-17) to tackle the issue of linearity of the response. Please see AC1 for a more general response with a simple linearity analysis.

7:19-25 The connection between these results and SSWs is unclear to me. As with the preceding paragraph, I don't think it belongs in the paper.
7:26-33 As noted in my major comments, the time evolution is extremely important. And the fact that this is not a climatological (converged) response makes the comparison with global warming even more tenuous.
Answer: Both paragraphs have been removed.

7:36 If I am not mistaken, the forcing is exactly 7 times stronger than in the 10box run. Is the anomaly approximately 7 time stronger?
Answer: We didn't check this as it makes a little sense to compare these two runs (SSWbox and 10box). With certainty we can say that the response to the strongest injection of -70 m/s/day in our SSW simulations is fully nonlinear, as it contains creation of new pressure structures etc.

7:34-8:5 The authors need to show the time evolution here if they want to relate this to a SSW. How sudden is the warming? Is it simply a massive gravity wave drag destroying the vortex, or does the resolve circulation play a role in the break down of the vortex. [All this said, I'm not sure how relevant this simulation is to the real world, or to the key conclusions of this paper.]
Answer: The time evolution is shown in Fig. 4 in the revised manuscript. We didn't analyze the SSWs in detail, because this would be worth a single paper (leaving it for near future), but from Fig. 8 it seems clear that anomalous PWs play a leading role.

8:5-7 What is the vertical extent of the gravity wave driving? I presume that it does not extend to 60 km.
Answer: The artificial GWD extends from approx. 20 to 30km.

8:8-11 I'm willing to accept this is as the best default run, but I was not convinced by the discussion here. If the response is linear, then it's trivial to chose an integration. If it is not linear, then it would be good to give more motivation why this is the best case.
Answer: We are now giving a detailed argumentation why the Box0.1 simulation is chosen for majority of analyses at P5L20-30.

8:25-26 Why is this unexpected. If I understand correctly, the net acceleration of the imposed gravity wave drag is constant in height. But since there is more mass lower in the atmosphere, the effective drag is much larger at the bottom (more precisely, the net force will be proportional to pressure).
In Fig 4, I believe the authors scale the E-P flux divergence as net force, so I'd expect the response to be largest at the bottom – this is simply where perturbation force is

largest. (I suspect the response is in part a compensation, as explored by Cohen et al. 2013,14.)
Answer: This has been explained by one of the referees already during the review process to ACPD and it is not present in the ACPD version.

8:27-29 Note that the E-P fluxes are really just a diagnostic. They don't establish causality. Thus it might be better to say "The anomalies are associated with a stronger poleward ...
To establish causality, you would need to explain why the waves propagate more strongly poleward.
Answer:We are using now "is associated with", where the causality is not clear.
However, the section 3.2 has been significantly rewritten and now we are giving more evidence for generation of PWs by the GWD region.

9:2-5 As noted above, it is clear that the gravity wave drag caused these changes in wave propagation (you compare with and without gravity wave drag). But it's not clear to me why this is happening?
Is it a compensating response? Or could it be interpreted with the index of refraction, that the deceleration by the gravity wave drag slows the winds, causing the resolved waves to shift and break in new places?
9:6-8 Why does this happen? Why do you need to presume that it creates poleward propagating PWs?
Answer: We are now identifying two acting mechanisms that create anomalies in the PW activity in the section 3.2: index of refraction and anomalous PW generation (absent for ring simulations).
We expect the box to create a large spectrum of waves and their modes, because it is an unbalanced force causing displacements in a balanced and predominantly zonal flow. This is now discussed at P10L9-14 .

General comment: there's too much discussion of supplementary material. If it's important, please include it in the paper.
Answer: The role od supplementary material has been diminished by the revisions we made.

9:15-17 "Probably" doesn't sound very scientific. What is the basis for this speculation? [And does the gravity wave deceleration extend below 35 km, or it confined above this level. If you think nudging is active here, then the response of the model is probably questionable.]
9:20 By total harmonic amplitude, do you mean the RMS amplitude? Or the mean square amplitude?
9:18-26 These figures suggest that the time evolution is quite complex, and that the simulations have not converged over 30 days. If the time evolution is important, it should be explored and discussed in more detail. It's not clear to my why, for example, you get a peak response at day 6.
Answer: This paragraph and the corresponding figure have been removed.

9:27-35 I believe that the inertial gravity waves generally don't have a period of 1 day. The frequency is related to the Coriolis parameter, and so a function of latitude. Gravity wave frequencies is bounded between the Brunt-Vaisala frequency

N and the Coriolis parameter f, with interial or near inertial waves coalescing at f = 2 omega sin (lat). At (for example) 50 N, it's 16 hours, and it will only will only be a day at a single latitude in the subtropics.
Answer: Thank you very much for pointing out this. For a detailed response please see the AC1. It is most likely a product of nonlinear interaction of inertia GWs and tides- P12L3-6.

More generally, why would you expect the forcing to radiative inertial gravity waves? There's definitely something odd here. If the forcing is causing instability, I'd be quite worried about the ability of the model to resolve it, given the coarse resolution.
Answer: As written above, we expect the GWD box to create displacements (both horizontal and vertical) and then it is up to the background which waves will be supported to propagate. Also inertia GWs long enough to be resolved are anomalously generated and can propagate even to the SH (revealed by power spectral differences of anomalous modal amplitudes between different latitude bands, not shown).

10:1-2 I do not understand this argument. Is the response really periodic on longer time scales? It's unclear from just a 30 day snap shot – and the solution doesn't seem to have converged to a periodic oscillation at either latitude.
A Hovmoller diagram would allow you to show the wave amplitude as a function of latitude and time, providing valuable information in the paper that is now in the supple- ment.
10:23-31 It is hard to follow or understand this discussion without more evidence. What is the evidence of wave reflection? Does it show up in a change in the vertical structure of the waves?
I'm curious how these anomalous waves related to the climatological waves. Is there positive or negative interference (see Fletcher and Kushner 2011)
Answer: This subsection has been removed.

11:22-27 The time evolution is very troubling, and not sufficiently document in the text.
Note also that the shallow branch of the residual circulation is generally associated with synoptic waves breaking on the top of the subtropical jet. Are there synoptic waves in your model? If you want to explore the residual circulation in more detail, I might sug- gest considering a downward control analysis. To what extent are the resolved waves amplifying or compensating the anomalies associated with the artificial drag? [You could include the nudging in this analysis: if it's not too strong, it might not overwhelm the response.]
11:28-12:20 I don't think it's appropriate to spend so much of the text discussing the supplement. If this is important, please hovmoller diagrams or other means to distill into a figure that can be included in the paper.
Answer: The entire Section 3 has been revised not to rely on the supplementary animations. We prefer to present the information on residual circulation using vectors (vres, wres) colored by the strength of the mass flux, because then certain features nicely emerge (lee wave pattern etc.).

Fig. 8. It was unclear to me how to relate this figure to the results shown in the paper. Are the authors arguing that there is enhanced subsidence is causing the enhanced ozone column? Is so, please show this.
12:34-13:5 I think it is quite a stretch to compare MUAM vertical velocity anomalies with MIPAS CH4. Why not start by comparing with the vertical velocity in a reanalysis, such as MERRA, which I believe extends pretty high in the stratosphere. Then you could compare the same quantity.
Answer: This subsection has been removed and the figures moved to the supplement to give motivation for the EA/NP research only.

13:34-35 What discrepancy? Do you mean the differences that are only shown in supplementary figures? The "SSW" run is an extremely nonlinear case, so I don't think you should expect it to be similar, and I'm not sure how relevant it is to the real world.
14:4-12 I do not really understand the discussion in this paragraph. What positive feed- back? I suspect gravity waves break in the EA/NP region because they are produced by flow over the Tibetan plateau and instability in the storm track. They break when they reach critical levels or become convective unstable. I don't see how the temperature in the region, however, would cause them to break.
14:33-38 This would be an interesting result, but I don't think the compensation argu- ment is really developed in the paper.
As noted in my major comments, I feel that the conclusions section become a narrative of open questions and interesting results in the field, but is not very much related to the results of the paper. This section needs to be reworked in detail. I think a shorter summary and discussion would make the paper more effective. (Overall I recommend using the conclusions section to review the key results of the paper and explain their broader context.)
Answer: We absolutely agree and the Discussion and conclusions section has been restructured, rewritten and a summary of results is now given at P14L30-P15L24.

Comments on figures: We have newly generated the figures according to the comments.

Influence of the spatial distribution of gravity wave activity on the middle atmospheric circulation and transport.

Petr Šácha[1], Friederike Lilienthal[2], Christoph Jacobi[2], Petr Pišoft[1]

[1]Department of Atmospheric Physics, Faculty of Mathematics and Physics, Charles University in Prague, V Holesovickach 2, Prague 180 00, Czech Republic

[2]University of Leipzig, Institute of Meteorology, Stephanstr. 3, 04103 Leipzig, Germany

Correspondence to: Petr Šácha(petr.sacha@mff.cuni.cz)

Abstract. Analyzing GPS radio occultation density profiles, we have recently pointed out a localized area of enhanced gravity wave (GW) activity and breaking in the lower stratosphere of the Eastern Asia/North-western Pacific (EA/NP) region. With a mechanistic model of the middle and upper atmosphere experiments are performed to study a possible effect of such a localized GW breaking region on the large-scale circulation and transport and, more generally, a possible influence of the spatial distribution of gravity wave activity on the middle atmospheric circulation and transport.

The results indicate an important role of the spatial distribution of GW activity for the polar vortex stability, formation of planetary waves (PW) and for the strength and structure of the zonal mean residual circulation. Also, a possible effect of a zonally asymmetric GW breaking in the longitudinal variability of the Brewer-Dobson circulation is analyzed. Finally, consequences of our results for a variety of research topics (sudden stratospheric warmings, atmospheric blocking, teleconnections and a compensation mechanism between resolved and unresolved drag) are discussed.

1 Introduction:

Consideration of gravity wave (GW) related processes is necessary for a proper description and modeling of the middle (as reviewed comprehensively by Fritts and Alexander, 2003) and upper atmospheric dynamics (see, e.g., the review by Smith, 2012). However, only recently satellite and other observational datasets with improved resolution and novel analysis methods together with high-resolution global models have been tightening the constraints for the parameterizations that can improve the treatment of these waves in climate models (Alexander et al., 2010; Geller et al., 2013).

Complex understanding and unbiased modeling of the middle atmospheric conditions is vital for climate research and there is strong evidence that coupling between chemistry and dynamics in the stratosphere is essential for surface climate variability and climate change in both hemispheres (Manzini et al., 2014; Calvo et al., 2015). There is also a wide recognition of dynamical links between the stratosphere and troposphere with a potential to significantly affect conditions at the surface (Haynes, 2005; Kidston et al., 2015). Hence, better representation of the stratosphere could improve the long-range and also short range forecast skills (Hardiman and Haynes, 2008; Gerber et al., 2012).

The Brewer–Dobson circulation (BDC) was first discovered based on the distribution of trace gases by Brewer (1949) and Dobson (1956). Using the transformed Eulerian mean equations, Dunkerton (1978)

Petr Šácha 18.10.16 13:37
Deleted: for

Petr Šácha 18.10.16 13:37
Deleted: (MUAM),

Petr Šácha 18.10.16 13:38
Deleted: also

Petr Šácha 18.10.16 13:38
Deleted: S

Petr Šácha 18.10.16 13:38
Deleted: S

Petr Šácha 18.10.16 13:38
Deleted: W

Petr Šácha 26.9.16 12:11
Deleted: In an early numerical attempt to demonstrate the importance of IGWs for the middle atmospheric dynamics, Holton (1983) concluded with formulating some requirements on GW related information (e.g. spatial and seasonal distributions of phase speeds, amplitudes etc.) to improve global climate model parameterization schemes.

Petr Šácha 26.9.16 12:14
Deleted: global

Petr Šácha 26.9.16 13:51
Deleted: Long-term and decadal changes of the middle atmosphere have been found to be largely owing to climate gas changes and thus reflect climate change (e.g. Lübken et al., 2013; Jacobi et al., 2015) yet it has been difficult to match observations with the robust model stratospheric change projections determined to a large extent by a speeding-up of the Brewer–Dobson circulation (BDC; Butchart, 2014; Kidston et al., 2015). Although weather systems are not able to penetrate into the stratosphere t

Petr Šácha 27.9.16 16:02
Deleted: B

Petr Šácha 26.9.16 14:15
Deleted: (Hardiman and Haynes, 2008)

derived a first dynamically consistent two-dimensional picture of the mean-transport streamlines for the middle atmosphere that is often used as a basic BDC concept. However, Demirhan Bari et al. (2013) found a 3D structure of the circulation in the middle atmosphere to be in good correspondence with tracer fields, especially in relation to the zonal wave-one pattern observed in the stratosphere and mesosphere, although their study did not give a comprehensive dynamical explanation of the discovered circulation structures (enhanced downward branch of BDC over north-eastern Asia, wave-one pattern).

PWs are usually thought to be created in the troposphere and then vertically propagating into the middle atmosphere. The theoretical possibility of PW creation by zonally asymmetric IGW breaking was first numerically analyzed by Holton (1984) and later on, e.g., by Smith (2003) and Oberheide et al. (2006), and experimentally verified by Lieberman et al. (2013). There is a building agreement in the literature on the role of wave activity in preconditioning sudden stratospheric warming (SSW; e.g. Ayarzaguena et al., 2011) events.

SSWs belong to the most pronounced atmospheric phenomena, as they cause abrupt changes of middle atmospheric circulation and tracer distribution, and they also affect tropospheric weather patterns (e.g. Manney et al., 2009; Kuroda, 2008; Lehtonen and Karpechko, 2016). SSW dynamics and their impacts differ whether a split or a displacement of the stratospheric polar vortex takes place (Seviour et al. 2016.) and it has been observed that displacements are connected with a dominating wave-one activity while vortex splits correlate with stronger wave-two activity (e.g., Kuttippurath and Nikulin, 2012). Generally, most attention is paid to the role of upward propagating PWs preconditioning SSWs (Hoffmann et al., 2007; Nishii et al., 2009; Alexander and Shepherd, 2010).

The two open questions regarding the dynamics of SSWs are: what types of wave phenomena are responsible for the SSW triggering and what are the necessary basic state conditions? There are two main triggering theories discussed - anomalous tropospheric upward wave fluxes or nonlinear resonance in connection to the vortex geometry (Albers and Birner, 2014). Also, there is growing observational evidence that GW amplitudes are enhanced prior to SSWs (Ratnam et al., 2004a; Wang and Alexander, 2010; Yamashita et al., 2010), and GWs are acknowledged to play a role in a wide range of SSW related processes (e.g. mesospheric cooling, stratopause separation and recovery Dunkerton and Butchart, 1984; Richter et al., 2010; Limpasuvan et al., 2012; France et al., 2013; Chandran et al., 2013; Siskind et al., 2010; Albers and Birner, 2014).

However, when the GW-PW interaction is consedered, the majority of studies are concerned by the modulation of GWs by PWs (e.g. Cullens et al., 2015) and about the GW impact on the upper stratosphere/mesosphere region. Šácha et al. (2015) indicated a possible GW breaking in the lower stratosphere. Indeed, model experiments with gravity wave drag (GWD) parameterization showed that orographic GWD in the lower stratosphere can significantly affect the development of SSWs (Pawson, 1997; Lawrence 1997) and the large scale flow in the lower stratosphere and troposphere in general (McFarlane, 1987; Alexander et al., 2010; Sandu et al., 2016).

McLandress et al. (2012) found changes of PW drag resulting from artificial enhancements of the orographic GW sources in the parameterization. This was called a compensation process and was

Petr Šácha 26.9.16 14:41
Deleted: now generally considered... [1]

Petr Šácha 26.9.16 14:34
Formatted: Czech

Petr Šácha 27.9.16 16:03
Deleted: then... e.g., by Smith (2003) ... [2]

Petr Šácha 26.9.16 14:51
Deleted: ...SWs events ...elong to th ... [3]

Petr Šácha 27.9.16 11:59
Deleted: I...W amplitudes are enhanc ... [4]

Petr Šácha 18.10.16 13:39
Deleted: On the other hand...,...the r ... [5]

Petr Šácha 27.9.16 16:22
Deleted: Recently, artificially enhancing the GWD by modifications of the orographic wave sources in the parameterization McLandress et al. (2012) found that the extra GWD results in changes of PW drag.

further statistically confirmed by Cohen et al. (2013), who interpreted it as a response of the resolved waves to maintain a ''sensible'' stable circulation. Such a response is expected, since all processes in the atmosphere are driven by the tendency to reach an energetically more favorable, stable state. In addition to the stability constraint, Cohen et al. (2014) proposed two additional mechanisms using a potential vorticity (PV) concept, PV mixing and refractive index interaction.

In this study, we focus on the physical mechanism and structure of the atmospheric response to the zonally asymmetric forcing represented by an artificially injected GWD in the stratosphere. We are following Šácha et al. (2015), who described a localized area of enhanced GW activity and breaking in the lower stratosphere over the Eastern Asia/North-western Pacific (EA/NP) region and discussed possible implications of this GW hotspot for large scale dynamics and transport. By artificially enhancing the GWD in a 3D mechanistic circulation model of the middle atmosphere, we examine the hypothesis that such a robust breaking region plays a role in forcing longitudinal variability of the BDC and can generate PWs. Further, we investigate possible implications for the polar vortex stability and the role of the GWD distribution and of the artificial forcing components (direction of the force).

The structure of the paper is as follows: in section 2 we describe the model and sensitivity simulation set up together with the observational motivation and justification for an artificial GWD enhancement. The section closes with a brief description of tracer data used in this study. Section 3 starts with an illustration of the geopotential response to different GWD injections with particular focus on effects in the polar region. We also present the dynamical impact, structure and modes of the PWs generated by the artificial GWD. Finally, we show the differences of the BDC due to the geometry of the GWD modulation and analyze the 3D residual circulation spatial patterns in relation to the GWD distribution. In Section 4, we give a summary of our results, discuss potential implications of our findings and outline future directions of our work.

2 Data and methodology

2.1 Model description and configuration

We use the Middle and Upper Atmosphere Model (MUAM), which is a nonlinear 3D mechanistic global circulation model. It has a horizontal resolution of 5°x5.625° and extends in 56 vertical layers up to an altitude of about 160 km in log-pressure height (Pogoreltsev et al., 2007). At 1000 hPa, the lower boundary of the model, we prescribe stationary PWs of wave numbers 1, 2 and 3 obtained from decadal monthly mean ERA Interim (ERAI) temperature and geopotential reanalysis data (ECMWF, 2016). Up to an altitude of 30 km the model zonal mean temperature is nudged to ERAI zonal mean temperature. This is necessary because MUAM does not account for, e.g., orography or some radiative processes including 3D water vapor or surface albedo. However, the troposphere is necessary for stationary PW forcing and the generation and propagation of traveling PWs and tides and therefore it cannot be neglected. The assimilation of stationary PWs and zonal mean temperatures is not only active during the spin-up of 330 model days but also during the 30-day analysis period.

The effect of nudging during the analysis period is dependent on the strength of the artificial forcing. In the reference simulation the nudging effect is lower than 1 K/day everywhere and for the simulation

Petr Šácha 27.9.16 16:23
Deleted: energetically

Petr Šácha 27.9.16 16:23
Deleted: paper

Petr Šácha 18.10.16 13:41
Deleted: (MUAM; Pogoreltsev et al., 2007)

Petr Šácha 27.9.16 16:26
Deleted: of distribution

Petr Šácha 27.9.16 16:26
Deleted: e

Petr Šácha 18.10.16 13:41
Deleted: a

Petr Šácha 27.9.16 16:27
Deleted: in

Petr Šácha 27.9.16 16:28
Deleted: geometry

with strongest forcing it reaches locally to magnitudes around 2 K/day in a zonal mean (as shown in Fig. 1c). Because in MUAM simulations only the zonal mean temperatures are nudged to the zonal mean, nudging has no direct effect on the wave structure of the response to the forcing, but is likely to reduce the magnitude of the zonal mean response.

The time step of the model is 225 s following a Matsuno (1966) integration scheme. For simulations, the model starts with a globally uniform temperature profile and no wind. During a spin-up period, the mean circulation is built, and PWs and tides are generated. After that, a time interval of 30 model days with a temporal resolution of 2h is analyzed. Since the lower boundary conditions are taken as a decadal mean January mean, this interval refers to an average January climatological state. Monthly zonal means of wind, temperature and GWD are given in Fig. 1. Owing to the constant forcing with time in the lower atmosphere, the standard deviation of temperature within these 30 days is smaller than 3K near the stratopause and mesopause and smaller than 1K elsewhere. The standard deviation of the zonal wind is largest within the jets reaching 4 m/s in the summer easterlies. These values do not have a meteorological meaning and are provided here to demonstrate that MUAM has a rather small variability within the analysis interval.

GWs are parameterized after a linear Lindzen (1981) type scheme updated as described in Fröhlich et al. (2003) and Jacobi et al. (2006), and they are initialized at an altitude of 10 km with six different phase speeds ranging from 5 to 30 m/s, each propagating in eight different azimuth angles, and with GW vertical velocity amplitudes with an average value of 0.01 ms^{-1}. As input for the GW parameterization scheme, we modified the GW source function to reflect a distribution based on the mean January field of the potential energy of disturbances computed from FORMOSAT3/COSMIC radio occultation density profiles between the tropopause and 35 km altitude taken from Šácha et al. (2015). The GW weights are calculated from these data by dividing the potential energy at each grid point by its global mean. This setup has a positive impact on some climatological features in MUAM. Nevertheless, the effect on the horizontal distribution of GWD in the stratosphere is negligible. We will refer to this setup as the reference simulation. Zonal (*gcu*) and meridional (*gcv*) flow acceleration as well as the heating due to breaking or dissipation of GWs (*gt*) is calculated by the parameterization scheme.

To examine and to demonstrate the effect of spatial distribution of the GW activity we performed a set of sensitivity simulations (Table 1) with artificially changed GWD imposed on the model by modulating the GW parameterization output. Note that this change of GWD is only added after the spin-up so that only the 30 model days incorporate GWD changes. Thus, the simulation period also includes the temporally delayed response for the adaption from reference conditions to enhanced GWD (*gcu/gcv/gt*) values. The naming convention (Table 1) is given by "Gcu+distribution+gcv", where the basic value of *gcu* of 0.5 m/s/day is not stated .

The enhancement is performed for a certain 3-dimensional box in the lower stratosphere (about 18-30 km) above the EA/NP region (37.5-62.5°N/112.5-168.8°E), according to the area of enhanced GW activity described by Šácha et al. (2015). This refers to the “box” distribution in Table 1 (an example is shown in Fig. 2, left panel). There are no exceptional GWD values in the reference simulation in this

Petr Šácha 11.10.16 10:45
Deleted: We use the Middle and Upper Atmosphere Model (MUAM), which is a nonlinear 3D mechanistic global circulation model. It has a horizontal resolution of 5 × 5.625° and extends in 56 vertical layers up to an altitude of about 160 km in log-pressure height as described by Pogoreltsev et al. (2007). At 1000 hPa, the lower boundary of the model, we introduce stationary PW of wave numbers 1, 2 and 3 obtained from ERA Interim (ERAI) temperature and geopotential reanalysis data (ECMWF, 2016). Up to an altitude of 30 km the model zonal mean temperature is nudged to ERAI zonal mean temperature to correct the climatology in the troposphere. This assimilation of stationary PWs and zonal mean temperatures is not only active during the spin-up but also during the analysis period. The time step of the model is 225 s following a Matsuno (1966) integration scheme. For simulations, the model starts with a globally uniform temperature profile and no wind. During a spin-up period, the mean circulation is built, and stationary PW a ... [6]

Petr Šácha 11.10.16 10:47
Deleted: GWs are parameterized after a linear Lindzen (1981) type scheme upd ... [7]

Petr Šácha 18.10.16 13:44
Formatted: Superscript

Petr Šácha 12.10.16 14:21
Deleted: an

Petr Šácha 12.10.16 14:21
Deleted: a

Petr Šácha 12.10.16 14:21
Deleted: y

Petr Šácha 12.10.16 14:21
Deleted: a

Petr Šácha 18.10.16 13:49
Formatted: Font:Italic

Petr Šácha 18.10.16 13:49
Formatted: Font:Italic

Petr Šácha 18.10.16 13:49
Formatted: Font:Italic

Petr Šácha 18.10.16 13:49
Deleted:)

Petr Šácha 18.10.16 13:49
Formatted: Font:Italic

Petr Šácha 12.10.16 14:22
Deleted: s

Petr Šácha 18.10.16 13:49
Formatted: Font:Italic

Petr Šácha 18.10.16 13:49
Deleted:

Petr Šácha 18.10.16 13:50
Formatted: Font:Italic

Petr Šácha 11.10.16 13:50
Deleted: 1

region. In a second version we additionally averaged the respective GWD parameters zonally within the same latitude range like the box. This way, we obtain a zonally uniform distribution, i.e. a ring of enhanced GWD parameters instead of a box but with a smaller local magnitude. We refer to this configuration as ring or "Zon" simulations (see Table 1). For all simulations, the GWD parameters outside the box or the ring, respectively, remain unchanged and are not influenced by the enhancement. We are not smoothing the boundaries of the artificial enhancement area and the step between artificial and background GWD values is dependent on the horizontal location, the time step and, most importantly, the altitude level. To illustrate the sudden and localized effect of GW breaking, we have chosen to enhance the GWD in our simulations stepwise and rather abruptly. As suggested by Cohen et al. (2013), such a sharp change (as at the boundaries of our enhancement) leading to dynamic instabilities is likely to induce compensation processes.

Although it is impossible to directly compute the GW drag force from current satellite measurements alone (Alexander and Sato, 2015), Ern et al. (2011) gave a methodology to estimate absolute values of a "potential acceleration" caused by GWs (maximum zonal mean values of 3 m/s/day below 40km). Using ray tracing simulations Kalisch et al. (2014) estimated a zonal averaged GWD to be around 20 m/s/day in the lower stratosphere. In our model simulations we are injecting three values of additional artificial zonal component of GWD, -0.5 m/s/day as a conservative enhancement and -10 m/s/day to demonstrate a big impact of the injection. In addition, an extreme case with -70 m/s/day is added to force substantial circulation changes.

Depending on the GW type and on the direction of background winds the GWD has also a meridional component, which is usually poorly constrained by observations. We performed simulations with three different values of meridional GW induced acceleration (-0.5 m/s/day, -0.1 m/s/day, 0.1 m/s/day). Directions of the zonal and meridional GW induced acceleration were chosen based on the assumption that the majority of GWs in the EA/NP region in January will be of orographic origin and taking into account the prevailing directions of horizontal winds in the EA/NP region (see Šácha et al., 2015). On this basis we argue that the 5:1 ratio between the zonal and meridional GW induced acceleration is the most realistic and therefore we choose the Box0.1 (and Zon0.1) simulation as a representative conservative enhancement for most of the analyses in this paper. A comprehensive discussion of our sensitivity simulation set-ups is given in the Discussion section.

2.2 Residual circulation

To highlight the importance of the stratospheric research in the EA/NP region and to show the robustness of our claim of an enhanced branch of the BDC in this region we present in the Supplement the 1978 to 2008 average total ozone January mean distribution from the ozone Multi Sensor Reanalysis version 1 (MSR1; van der A et al., 2010) data (TEMIS, 2016). Additionally, in the Supplement, the comparison is shown between the vertical structure and longitudinal variability of the residual circulation and zonal cross sections of Michelson Interferometer for Passive Atmospheric Sounding (MIPAS) CH_4 volume mixing ratio profiles (KIT, 2016; see von Clarmann et al., 2009; Plieninger et al., 2015). However, the interpretation of the differences of the distributions must be done with care, since the tracer distributions result from several different processes in the atmosphere,

Petr Šácha 27.9.16 14:43
Deleted: Our motivation for imposing an artificial drag stems from the findings of Šácha et al. (2015), who showed a localized area of enhanced GW activity and breaking in the lower stratosphere of the EA/NP region. In our sensitivity simulations we imitate the impact of the EA/NP lower stratospheric IGW breaking, which is not covered by the MUAM GW parameterization in the reference simulation ... [8]

Petr Šácha 27.9.16 15:13
Deleted: ... [9]

Petr Šácha 27.9.16 15:05
Deleted: 3

Petr Šácha 27.9.16 15:21
Deleted:

Petr Šácha 27.9.16 15:21
Deleted: as a representative and realistic conservative GWD enhancement.

Petr Šácha 3.10.16 16:20
Deleted: Tracers

Petr Šácha 27.9.16 15:43
Deleted: It is difficult to evaluate model results for large-scale stratospheric vertical velocities, as these are much smaller than horizontal velocities. Therefore,

Petr Šácha 27.9.16 15:47
Deleted: induced by the different configuration and distribution of GWD is compared with

Petr Šácha 27.9.16 15:49
Deleted: Further, to show the robustness of our claim of an enhanced branch of the BDC in the EA/NP region we computed the 1978 to 2008 average total ozone annual cycle from the ozone multi sensor reanalysis version 1 (MSR1; van der A et al., 2010) data (TEMIS, 2016).

namely advective transport, mixing, and chemical reactions (Garny et al., 2014). Also, the residual velocities are closely related to Lagrangian-mean velocities up to $O(\alpha^2)$ only for small amplitude (α) steady waves (Bühler, 2014).

In the section 3.3, we study consequences of the GW hotspot for the longitudinal variability of the residual circulation (and BDC consequently) by means of the time mean 3D residual circulation according to Kinoshita and Sato (2013). The time averaging inserts additional uncertainty in the 3D residual circulation concept. Unlike Demirhan Bari et al. (2013), who based their analysis on monthly means and daily eddies, we are employing a 5-day running average on the 6 hourly MUAM output fields. This configuration gives the strongest zonally averaged Stokes drift from several choices of the running mean. But, it is still smaller than the value of the Stokes drift resulting from transformed Eulerian mean equations, which is computed in this study according to Hardiman et al. (2010) for log-pressure height vertical coordinate models.

3. Results

To establish the timescales of the response, in Fig. 3 we show Hovmöller diagrams of the zonal mean zonal wind and its variance. The time evolution is presented at the 6.25 hPa level (around 35.5km log-pressure height, 13th model level). This level was chosen for our analyses because it is above the location of the artificially modified area and above the nudging extent, so it contains the atmospheric response only. In Fig. 3a, a Hovmöller diagram is given for the zonal mean zonal wind at 6.25 hPa level in the Ref simulation documenting that the model is essentially steady. Fig. 3b shows the time evolution of variance of the zonal mean wind anomaly (Box0.1-Ref) and Fig. 3c shows the time evolution of zonal mean zonal wind for the 10box simulation. We can see the buildup of the response until approx. day 7 after the GWD injection and after that the structure of the response remains quasi-steady, with small variations of the magnitude only.

In contrast to this, the zonal mean zonal wind time evolution from the so-called SSW simulations (Fig. 4a and 4b) do not reach a steady state in the course of the 30 days simulation and therefore the results based on those simulations are presented at particular time steps or as animations in the Supplement. Results of other simulations (Table 1) are averaged across the quasi-steady state (7th-30th day of the simulation) and are supplemented with the estimate of statistical certainty or standard deviation of the mean.

Except for the SSW simulations, our study is focused mainly on the mean response to a monthly mean GWD distribution, because from observational analyses we usually have information on the IGW activity distribution on a monthly or seasonal basis (Šácha et al., 2015). The short-term response, which would be arguably more relevant to the real atmosphere taking into account the intermittency of large amplitude GWs (e.g. Hertzog et al., 2012; Wright et al., 2013), is not well captured by the mechanism of constant GWD injection, which will be discussed in the final section. Still, there are some interesting results mentioned in the course of the study, e.g. note the agreement with the time scale of the transient response build up in Fig. 11d of Cohen et al. (2014), where it is related to the life cycle of the PW breaking.

Petr Šácha 27.9.16 15:51
Deleted:
Petr Šácha 27.9.16 15:51
Deleted: W
Petr Šácha 27.9.16 15:52
Deleted: In contrast to
Petr Šácha 27.9.16 16:33
Deleted: For t
Petr Šácha 27.9.16 16:34
Deleted: the
Petr Šácha 27.9.16 16:35
Deleted: gives subjectively most reasonable values
Petr Šácha 27.9.16 16:37
Deleted: w
Petr Šácha 27.9.16 16:38
Deleted: e
Petr Šácha 4.10.16 16:00
Deleted: compared to the
Petr Šácha 4.10.16 16:00
Deleted: residual circulation
Petr Šácha 5.10.16 13:06
Formatted: Normal, Justified, Line spacing: 1.5 lines

3.1 Atmospheric response to variations in GWD and SSW

Fig. 5(1A) shows the mean (7th-30th day) horizontal wind and geopotential field at the 6.25 hPa level (13th model level) for the Ref simulation and the remaining plots in the first row show anomalies (i.e. differences from the results of this run) caused by different components of GWD with artificial values corresponding to the Box0.1 simulation. The second row (Fig. 5(2A) – Fig 5(2D)) shows horizontal wind and geopotential anomalies for the 10box (Fig. 5(2A)) and Box0.1 (Fig. 5(2B)) simulations and differences between simulations with conservative GWD enhancements (Figs. 5(2C) and 5(2D)). The third row (Figs. 5(3A) through 5(3D)) shows the same as the 2nd row, but for the artificial ring GWD configuration. Note the different scaling of the color bars, which is chosen according to the maximal and minimal value of geopotential (anomaly), so that the labels of the color bar give direct information on the magnitude of the differences in geopotential response.

The anomalies and differences are analyzed with special focus on the polar vortex response, since it will be shown below that the dynamical response on GWD changes is strongest in the polar region. This comparison demonstrates not only the importance of the role of the longitudinal distribution of the zonal mean drag force but it also highlights an important and different effect of each of the individual GWD components.

From comparison of Figs. 5(1B), 5(1C), and 5(1D) we see that among the GWD components modified in the Box0.1 simulation the response to the *gcu* component is the strongest. It induces a dipole structured anomaly with negative geopotential anomaly downwind from the region of GWD enhancement and positive anomaly north of this region (Fig. 5(1B)). The *gt* component alone induces a positive anomaly of smaller magnitude northward and upstream of the area (Fig. 5(1C)). In contrast to that, meridional drag induces a negative geopotential anomaly northward and downwind of the area, which has the smallest magnitude of all three components, but is still significant (Fig. 5(1D)).

The respective geopotential responses in the Box0.1gcv and the Box0.1gt simulations have almost exactly opposite features, as the positive *gt* enhances geopotential in the upwind and northward direction from the GWD region, while artificial northward deceleration has an opposite effect. Although we used a nonlinear model, the additivity of effects of different GWD components (Figs. 5(1B), 5(1C), and 5(1D)) seems to hold reasonably well as can be seen from the Box0.1 anomaly (Fig. 5(2B)), where the forcing constitutes of exactly these components. Also, the differences between simulations with different meridional drag (compare Figs. 5(2C) and 5(2D)) show the same pattern as induced by the meridional drag only (Fig. 5(1D)). The distribution of the response to the meridional component suggests that a box *gcv* enhancement in this geographical position can influence the geopotential response in the area of location of the Aleutian High.

Another two important results are visible from the comparison of the plots in the second and third row of Figure 5. Firstly, there are much bigger anomalies for the box enhancements (second row) than for the corresponding ring enhancements (third row). This is true locally as well as in the zonal mean (compare the sum of geopotential response given in the legend for Figs. 5(2A), 5(2B), 5(3A) and 5(3B)). In the box simulations (Figs. 5(2A) and 5(2B)) the response is typically dominated by a rather meridionaly oriented dipole pattern with a localized positive geopotential anomaly at the center of the

Petr Šácha 27.9.16 16:42
Deleted: Atmospheric…response t ... [10]

Petr Šácha 5.10.16 12:35
Deleted: 2…1A) shows the monthly ... [11]

Petr Šácha 3.10.16 16:22
Formatted: Font:Not Bold, Italic, Font color: Auto

Petr Šácha 3.10.16 16:23
Deleted: presents …ighlights an im ... [12]

Petr Šácha 4.10.16 15:32
Deleted: F…om a …omparison of F ... [13]

Petr Šácha 18.10.16 14:07
Formatted: Font:Not Bold, Italic, Font color: Auto

Petr Šácha 4.10.16 16:06
Deleted: anomaly …s the strongest. ... [14]

Petr Šácha 18.10.16 14:08
Formatted: Font:Not Bold, Italic, Font color: Auto

Petr Šácha 4.10.16 16:07
Deleted: This …ositive anomaly of ... [15]

Petr Šácha 3.10.16 16:27
Formatted: Font:Not Bold, Italic, Font color: Auto

Petr Šácha 5.10.16 12:37
Deleted: 2…1CD…). In contrast to ... [16]

Petr Šácha 3.10.16 16:27
Formatted: Font:Not Bold, Italic, Font color: Auto

Petr Šácha 4.10.16 16:14
Deleted: meridional drag only …Fi ... [17]

Petr Šácha 6.10.16 13:36
Deleted: …he respective geopotent ... [18]

Petr Šácha 4.10.16 22:01
Deleted: the …eopotential in the up ... [19]

Petr Šácha 4.10.16 22:01
Formatted: Font:Not Bold, Italic, Font color: Auto

Petr Šácha 18.10.16 14:11
Formatted: Font:Not Bold, Italic, Font color: Auto

Petr Šácha 4.10.16 21:17
Deleted: There are…nother two imp ... [20]

polar vortex and negative geopotential anomaly at the location of Aleutian High. In the correspondent ring simulations (Figs. 5(3A) and 5(3B)) the geopotential response is more zonally uniform.

Secondly, there are large and significant differences (50% or 25% of the magnitude of the anomaly) between box simulations with slightly different setups of the meridional drag (Fig. 5(2B) vs. Figs. 5(2C) and 5(2D), respectively), while this is not true for ring GWD enhancements (few percent; see Fig. 5(3B) vs. Figs. 5(3C) and 5(3D)). Unlike the box enhancements, ring enhancements are almost insensitive to the different versions of GWD in the meridional direction. The difference between Zon0.1, Zon0.5 and Zon0.1pos simulations is very small and not significant.

As noted above, the magnitude of the geopotential response is larger for the box enhancements than for the ring enhancements. For the Box0.1 simulation, the geopotential anomaly at the 6.25 hPa level reaches about 20 gpm in a monthly mean. The horizontal wind anomaly for the Box0.1 simulation (Fig. 5(2B)) reaches maximal values slightly below 1m/s. Anomalies for the 10box simulation (Fig. 5(2A), 20 times bigger eastward deceleration than for Box0.1) are almost exactly 20 times stronger and show a very similar dipole pattern. Although locally the difference between these two simulations may seem to be linear, this comparison is misleading, since both simulations (10box and Box0.1) have different ratio between the strength of GWD components. This means, for example, that the drag force has different orientation between these two simulations.

Unexpectedly, the box simulations lead to anomalies that would contribute to weakening rather than amplification of the Aleutian High. Based on the results and discussion of Šácha et al. (2015), who argued that the EA/NP hotspot (high GW activity already in October/November) may play a role in the onset of the winter circulation in the stratosphere in this region, we expected a positive contribution of the GWD response to the background climatology (e.g. contribution to the unusually hot temperatures in the stratosphere in the EA/NP region by induced subsidence).

In Figs. 4a and 4b we presented a time evolution of the zonal mean zonal wind at 6.25 hPa for the SSWbox and SSWzon simulations with signs of a wind reversal at polar latitudes at particular time steps suggesting an occurrence of a minor SSW. Now we show additional results from the SSWbox and SSWzon simulation in the form of animations of geopotential and horizontal wind field response at 6.25 hPa (Animation 1a and 1b in the Supplement) and a snapshot at 280 hours after the injection to show the response at a developed stage of the SSW. In response to a strong GWD increase in a box we observed a vortex displacement (Fig. 6a and Animation 1a in the Supplement) and in response to a strong GWD increase in a ring we obtain a vortex split like event (Fig. 6b and Animation 1b in the Supplement).

In the SSWbox simulation (Animation 1a), immediately after the spin-up period when the GWD starts to be artificially modified (injection of GWD), a geopotential ridge begins to form above the Northern Pacific (northward from the GWD area). This anomaly strengthens and shifts a little westward above Siberia, where, from approximately 5 days of the GWD injection, we observe an evolution of a pressure high. All the time the vortex is shifting towards the northern boundary of Northern America where it stays till the end of the simulation.

Petr Šácha 5.10.16 12:38
Deleted: 2 …2B) vs. Figs. 52…2C) ... [21]
Petr Šácha 4.10.16 21:18
Deleted: u
Petr Šácha 4.10.16 21:20
Formatted ... [22]
Petr Šácha 4.10.16 21:20
Formatted ... [23]
Petr Šácha 4.10.16 21:38
Comment [1]: This will be shifted ... [26]
Petr Šácha 4.10.16 22:23
Deleted: *This could be a result of n* ... [24]
Petr Šácha 3.10.16 16:30
Formatted ... [25]
Petr Šácha 4.10.16 21:51
Deleted: , which comprises a conser ... [27]
Petr Šácha 4.10.16 22:25
Formatted ... [28]
Petr Šácha 4.10.16 22:24
Deleted: about 30 gpm in the later t ... [29]
Petr Šácha 4.10.16 22:25
Formatted ... [30]
Petr Šácha 4.10.16 22:24
Deleted: on
Petr Šácha 4.10.16 22:25
Formatted ... [31]
Petr Šácha 4.10.16 22:24
Deleted: at 6.25 hPa (about 35.5 kn ... [32]
Petr Šácha 4.10.16 21:39
Deleted: , which is comparable in m ... [34]
Petr Šácha 4.10.16 22:25
Formatted ... [35]
Petr Šácha 5.10.16 12:38
Deleted: 2
Petr Šácha 4.10.16 22:25
Formatted ... [33]
Petr Šácha 4.10.16 22:25
Formatted ... [36]
Petr Šácha 4.10.16 22:31
Deleted: Contrary to our expectations
Petr Šácha 4.10.16 22:32
Formatted ... [37]
Petr Šácha 5.10.16 10:50
Deleted: se
Petr Šácha 4.10.16 22:32
Formatted ... [38]
Petr Šácha 6.10.16 13:30
Deleted: h
Petr Šácha 4.10.16 22:32
Formatted ... [39]
Petr Šácha 4.10.16 22:31
Deleted: interference
Petr Šácha 4.10.16 22:32
Formatted ... [40]
Petr Šácha 4.10.16 22:32
Deleted: with
Petr Šácha 4.10.16 22:32
Formatted ... [41]
Petr Šácha 4.10.16 22:45
Deleted: an …nduced subsidence). ... [42]
Petr Šácha 3.10.16 16:31
Formatted ... [43]
Petr Šácha 4.10.16 22:33
... [44]
Petr Šácha 5.10.16 12:46
Formatted ... [45]
Petr Šácha 5.10.16 12:44
Petr Šácha 5.10.16 12:46
Formatted ... [46]
Petr Šácha 5.10.16 13:06
Petr Šácha 5.10.16 12:46

In the SSWzon simulation we observe a slow (compared to the SSWbox simulation) creation of a pressure high above the Northern Pacific together with a high-pressure ridge above the Northern Atlantic. This pressure high is almost stationary (in contrast to the SSWbox) leading to the vortex split approximately ten days after the injection. This is a potentially very interesting result suggesting that a symmetric forcing favors vortex split and localized forcing favors displacement events, but the robustness of this claim needs to be tested in future work for various initial vortex states.

For illustration, in Figure 6 we show the geopotential field and horizontal wind speed 280 hours after the GWD injection, when the vortex split develops (Fig. 6b) and the vortex displacement is in its mature state (Fig. 6a). The vortex displacement event develops more quickly, as seen from comparison of Fig. 4a and 4b or from the animations 1a and 1b in the Supplement. However, both events have limited vertical extent, and do not disturb the entire vortex (only up to 60 km of log-pressure height; not shown).

3.2 Creation of planetary waves and dynamical impact

In this section we compare PW activity and amplitude structure of the leading PW modes between reference, box and ring simulations. We show results of the E-P flux diagnostics and Fourier transform (FT) analysis of geopotential anomalies.

Fig. 7 shows the mean (7th-30th day) E-P flux and its divergence for the Ref simulation (Fig. 7a), Box0.1 simulation anomalies (Box0.1-Ref; Fig. 7b), Zon0.1 simulation anomalies (Fig. 7c), the difference between the Box0.1 and Zon0.1 simulations (Fig. 7d) and mean mean E-P flux and its divergence for the 10box simulation (Fig. 7e) and respective anomalies (Fig. 7f). Note that we show the E-P flux divergence as a force per unit area (units $[kgm^{-1}s^{-2}]$), not as an induced acceleration (units $[ms^{-2}]$), as in Hardiman et al. (2010), because otherwise upper stratospheric and mesospheric effects would dominate the plots due to the density decrease with height. The statistical significance of the mean E-P flux divergence differences has been computed by a t-test and regions with p values < 0.05 are stippled.

In Fig. 7b, for the Box0.1 and Ref simulation differences, we find an anomalously weak E-P flux convergence (positive difference to the Ref simulation) centered at the equatorward flank of the GWD enhancement area and an anomalous convergence in a broad area around 60°N. This pattern is similar for the Zon0.1 simulation anomalies (Fig. 7c), but much weaker and with the anomalous convergence starting more poleward. It is also similar in the 10box simulation anomalies (Fig. 7f), but much stronger in magnitude (approx. 20 times). In all of those simulations, this anomalous pattern is limited in altitude and only slightly exceeds the vertical boundaries of the GWD area (especially in the polar region).

Taking into account the reference E-P flux field (Fig. 7a), the anomalies can be caused by two different mechanisms. The first one is an indirect mechanism, when the artificial GWD drag modifies the winds causing changes (with respect to the Ref simulation) in propagation conditions for PWs propagating from below (for more details on the refractive index interaction see Cohen et al. (2014). According to this mechanism, the E-P flux and its divergence anomalies and differences (Figs. 7b, c, d, f) would be

Petr Šácha 5.10.16 12:50
Deleted: , because the anomaly is approximately ten times stronger than in the 10box simulation. …n the SSWzon si ... [55]

Petr Šácha 5.10.16 13:00
Formatted: Font:Not Bold, Not Italic, Font color: Auto

Petr Šácha 6.10.16 17:23
Deleted: significantly …isturb the e ... [56]

Petr Šácha 3.10.16 16:35
Comment [2]: To už je řečeno v methodologii?

Petr Šácha 3.10.16 16:35
Formatted ... [57]

Petr Šácha 3.10.16 16:35
Formatted: Font:Italic

Petr Šácha 7.10.16 13:39
Deleted: ,…boxBox0.1…,…nd ... [58]

Petr Šácha 10.10.16 10:15
Formatted: Font:Not Bold, Font color: Auto

Petr Šácha 10.10.16 10:15
Deleted: height and zonal wind zonal

Petr Šácha 11.10.16 14:03
Deleted: 4…shows the monthly…m ... [59]

Petr Šácha 7.10.16 13:45
Deleted: the differences or anomalies would be dominated by upper stratospheric and mesospheric effects due to density decrease

Petr Šácha 18.10.16 9:52
Deleted: 4…b, for the Box0.1 and R ... [60]

Petr Šácha 7.10.16 14:30
Deleted: Putting together

associated with a stronger poleward and weaker/stronger upward propagation of PWs in the 10box/Box0.1 simulation along the northern edge the polar night jet in the northern part and northern boundary of the GWD area. The E-P flux divergence anomaly at the southern flank of the GWD would be associated with a suppression of upward and equatorward PW propagation elsewhere in the GWD region. But this mechanism fails to explain some features in Fig. 7, e.g. the E-P flux divergence emerging in the E-P flux field in the 10box simulation (Fig. 7e). Therefore, although the changes in the refractive index will definitely be present in the artificial GWD simulations, we have an indication that another mechanism is dominant.

This second mechanism is associated with the evidence given by Holton (1984) that a zonally asymmetric GW breaking possibly generates PWs in the mesosphere. In connection with that the artificial GWD enhancement in a box would cause displacements of fluid particles (in the initially balanced predominantly zonal flow) and thus generate a broad spectrum of waves of different types depending on background conditions and on the geometry of the drag region. We can find support for this mechanism from the E-P flux difference between Box0.1 and Zon0.1 simulation (Fig. 7d).

In the previous section, we have shown that the box enhancement induces a stronger zonal mean geopotential response than the corresponding ring enhancement. So we can assume that the first mechanism has bigger effect in the box simulations, which is true for the E-P flux divergence difference (Fig. 7d). However, regarding E-P flux vectors, Fig. 7d reveals that there are not only differences in magnitude between Box0.1 and Zon0.1 E-P flux anomalies, but also that the Zon0.1 simulation lacks the horizontal component of the anomalous E-P flux, with biggest differences in the latitudinal band encompassing the artificial GWD area. This latitudinal band is not significant in Figs. 7b,c and d, because the plotted t-test results are based on the difference of the E-P flux divergence (not on the magnitude of the E-P flux vector difference). From Figs. 7 b, d, f, we see that the anomalous PWs are generated at the southern flank of the GWD area and propagate predominantly northward (with a small downward component), where they cause anomalous convergence between 60°-80°N.

For the conservative Box0.1 simulation, the anomalies in the E-P flux divergence are about 5% of the reference values. Zon0.1 E-P divergence anomalies (Fig. 7c) reach only 1-2% of the reference values, locally. Anomalies of the 10box simulation (Fig. 7f) exhibit the same pattern as Box0.1 anomalies, but the magnitude is much stronger - more than 50% of the reference E-P flux divergence values. Therefore, we observe an influence of the 10box GWD enhancement also in the mean field in Fig. 7e, where the artificial GWD box demonstrates itself as an E-P flux divergence area on the southern flank of the GWD enhancement region. This is another supporting argument that the box enhancement generates PWs, with further evidence given below.

In Fig. 8, E-P flux diagnostics is presented at particular moments (1 and 5 days) after the GWD injection for the SSWbox and SSWzon simulations. The anomalous E-P fluxes in those highly nonlinear simulations absolutely overcome the reference fields, so that we can directly observe the generation and propagation of PWs generated by the artificial GWD. However, for these simulations the structure of the E-P flux divergence area changes with time and also the propagation directions of PWs created in this region are time dependent. So, we have chosen to present snapshots from the 1st and 5th day to demonstrate particular features of the box GWD enhancement. For interested readers, the full time evolution is given as Animation 2 in the Supplement.

In Figs. 8a, b, one can clearly see the generation of PWs by the box enhancement. Five days after the GWD enhancement (Fig. 8b), the E-P flux divergence region extends almost over the whole GWD area. Anomalous PWs propagate equatorward, poleward and upward with two major E-P flux convergence regions around 30° N and between 60° and 80° N. One day after the GWD injection (Fig. 8a), the E-P flux divergence area is located at the southern flank of the GWD and generates horizontally, southward propagating PWs only. In Fig. 8a, in the majority of the GWD region, we can see also the first mechanism (refractive index interaction) being active, as the GWD region influences propagation of PWs propagating from below. This is the most dominant effect of the ring enhancement (Fig. 8c, d), where in the SSWzon simulation we can hardly observe any anomalous PW generation and the dominant effect of this ring enhancement is altering the propagation conditions for the upward propagating PWs from the troposphere. There is a weaker propagation through the GWD region, with deflection of PWs northward and southward at the southern GWD flank.

Further indication of the creation of PWs by the GWD region is provided by the FT analysis of geopotential anomalies at the 6.25 hPa level. FT provides information about the representation of different harmonics in the anomalous wave activity revealed by the E-P flux diagnostic and about the spatiotemporal distribution of their amplitudes. The mean (7th-30th day) latitudinal structure of reference amplitudes of leading PW modes is given in Figs. 9a, b. Anomalous amplitudes (Box0.1-Ref simulation) are presented in Fig. 9c, d and differences from the Zon0.1 simulation are shown in Fig 9e, f. To quantify the dispersion of the monthly mean differences, the dotted lines show the standard deviations.

The wave-1 geopotential amplitude is anomalously enhanced for a box GWD (Box0.1-Ref; Fig. 9c). The amplitude anomaly is positive starting at the northern flank of the artificial GWD (37.5-62.5°N) and further poleward. The maximum is gained between 70-75°N. Another smaller, but still significant, region of positive wave-1 amplitude anomaly is located around 30°N south of the GWD. Smaller negative wave-1 amplitude anomaly lies inside the GWD area. In the Box0.1 simulation, wave-2 (Fig. 9c) has a pronounced negative amplitude anomaly inside the latitudinal belt encompassing the enhancement region. For wave-3 (Fig. 9d), we find positive anomalous amplitudes starting from central latitudes of the GWD region and ending around 80°N, although inside the GWD region the positive anomaly is locally not significant. There is a negative wave-3 amplitude anomaly starting at the southern flank of the GWD region with the end around 10°N. The effect on wave-4 amplitudes is almost negligible (Fig. 9d). The ring enhancement in the Zon0.1 simulation has a negligible effect on amplitudes of harmonics, as is visible from the similarity of the Box0.1 anomalies (Figs. 9c, d) and differences with Zon0.1 simulation (Figs. 9e,f). These results suggest that the box GWD enhancement generates preferentially wave-1 and -3 modes in comparison to the reference and also the ring GWD configuration.

Another indication that the PWs are indeed generated by the GWD box enhancement is given in Fig. 10, where the time evolutions of the anomalous wave-1 and wave-3 amplitudes are presented.

Petr Šácha 7.10.16 15:10
Deleted: in Fig. 4b with a full field from the Ref simulation (Fig. 4a), we see that the Box0.1 anomalies are due to a stronger poleward and also upward propagation of PWs along the northern edge of the jet from the northern part of the GWD area, and due to a suppression of upward and equatorward propagation elsewhere in the GWD region. South of 30°N only, there is a small area of anomalous convergence due to the anomalous equatorward propagation from the GWD area. For this conservative Box0.1 simulation the differences in the E-P divergence are around 5% of the reference values. In contrast to that, Zon0.1 E-P divergence anomalies reach only 1 or 2% of the reference values, locally. These results confirm that the localized forcing has a potential to modify PW activity more efficiently than a zonally uniform drag of the same zonal mean zonal force. ... [61]

Petr Šácha 6.10.16 17:43
Formatted: Font:Not Bold, Italic, Font color: Auto

Petr Šácha 11.10.16 22:31
Formatted: Space After: 0 pt

Petr Šácha 11.10.16 13:33
Deleted: zonal …eopotential and zo ... [62]

Petr Šácha 11.10.16 22:46
Formatted ... [63]

Petr Šácha 11.10.16 22:37
Deleted: different …eading PW mo ... [64]

Petr Šácha 12.10.16 11:15
Deleted: w

Petr Šácha 12.10.16 11:10
Formatted: English (AUS)

Petr Šácha 12.10.16 11:07
Deleted: y…for a box GWD (betwe ... [65]

Petr Šácha 12.10.16 11:04
Deleted: erence… ... [67]

Petr Šácha 12.10.16 11:10
Formatted: English (AUS)

Petr Šácha 12.10.16 11:10
Formatted ... [66]

Petr Šácha 12.10.16 11:10
Formatted ... [68]

Petr Šácha 12.10.16 11:07
Deleted: and the difference between box and ring simulation reach…s positive a ma ... [69]

Petr Šácha 12.10.16 11:10
Formatted: Font:(Default) Times New Roman, English (AUS)

Petr Šácha 12.10.16 11:13
Deleted: , and a minimum around the northern part of …ies inside the GWD ... [70]

Petr Šácha 12.10.16 11:13
Formatted: English (AUS)

Especially in the first approximately seven days from the GWD injection, we can observe a slow propagation of anomalous wave-1 (Fig. 10a) and wave-3 (Fig. 10b) amplitudes from the GWD region to the north. For wave-3 this propagation is visible later than for wave-1 (from approx. day 3). The oscillating patterns in Fig. 10 most likely originate from a non-linear interaction between anomalously generated inertia GWs and solar tides (see e.g. Waltersheid, 1981). Those inertia GWs are responsible for propagation of the anomalous wave activity through the Rossby wave critical layer in the tropics, across the equator, and into the Southern Hemisphere (Fig. 11).

3.3 Residual circulation response

The first row of Fig. 11 shows the mean (over the whole 30days) residual circulation mass fluxes for the reference simulation and the snapshot at 5days from the GWD injection for SSWbox simulation on the right. Mean (7th-30th day) anomalies and differences with the respective ring configuration are given in the second and third row for the Box0.1simulation on the left and 10box simulation on the right. There are some remarkable results visible. Firstly, even for a conservative drag enhancement (Box0.1 simulation) there are significant (dashed) differences in the magnitude of the residual mass flux between box and ring GWD distribution of up to 3% in the lower stratosphere (Fig. 11e). For the 10box simulation the differences reach about 40% and create a similar pattern as for the conservative enhancement (Fig. 11f). The largest differences between the two artificial GWD configurations are found poleward from the GWD enhancement region in the altitude range between 20 and 30 km corresponding approximately to the vertical extent of the area and are associated with a stronger subsidence north of the enhancement region in the box simulations.

There is a smaller region of significant differences at the southern flank of the enhancement region associated with lesser downwelling in the box simulations. These two regions of significant differences constitute together a butterfly like pattern in the box-ring differences centered at approximately 45°N (the center of the enhancement region) and influencing a shallow BDC branch. Taking into account the reference field (see Fig. 11a) we can explain this pattern by a faster northward advection starting at approx. 45°N and stronger subsidence northward of 60°N. On the other hand there is less upwelling in the equatorial region (not significant for the Box0.1 simulation) and slower advection from the tropics. The continuity is satisfied through smaller downwelling south of 60°N.

We observe a similar but stronger pattern in the anomalies (Figs. 11c, d), with the mean residual circulation mass flux anomaly reaching up to 5% for the Box0.1 simulation and more than 60% for the 10Box simulation. The position of the anomalous residual circulation patterns corresponds with the E-P flux divergence anomalies (Fig. 7b, f), where, for the box simulations, we observed anomalous E-P flux divergence at the southern flank and convergence north of the GWD region. In Figs. 11c and 11d the butterfly like pattern is centered more southward (35°N) than in box-ring differences and the anomalous pattern on the south of the GWD region is not as well pronounced and appears to be shifted above the GWD region for the 10box simulation (Fig. 11d).

In the upper stratosphere there are anomalies up to 2% only for the Box0.1 (Fig. 11c) and locally around 25% for the 10box simulation (Fig. 11d). The box simulations (not significant for Box0.1) show

Petr Šácha 12.10.16 14:08
Formatted: English (US)

Petr Šácha 12.10.16 14:09
Deleted: We are enclosing an animation of the time evolution of the latitudinal structure in the Supplement (Animation 2), where one may see the slow buildup of anomalous wave amplitudes due to the PW activity northward from the GWD area and the propagation of anomalies into the SH, and pulsation of the amplitude maxima due to inertia GWs ... [71]

Petr Šácha 19.10.16 10:28
Deleted: F…rst row of Fig. 11 7 … ... [72]

Petr Šácha 13.10.16 10:33
Deleted: differences…are slightly ... [73]

Petr Šácha 13.10.16 10:47
Deleted: anomalous fields…nomali ... [74]

Petr Šácha 13.10.16 11:20
Formatted: Font:(Default) +Theme Body, Czech

Petr Šácha 13.10.16 11:22
Deleted: the anomalous fields (…ig ... [75]

Petr Šácha 13.10.16 13:02
Deleted: differences and

weaker subsidence towards the polar vortex center than the Ref simulation in the upper stratosphere and there is also anomalously low mass flux poleward and downward between 30 and 40 km of height above the GWD enhancement region. For both box enhancements, there is a large area of statistical significant anomalies giving a weak hint of lesser upwelling in the SH stratosphere (Figs. 11c, d). The differences between the two sets of box and ring GWD configuration are not significant in the SH (Figs. 11e, f).

The fact that the mean response of the upper BDC branch is rather weak and for the most part not significant can be explained by the effect of the artificial GWD region acting like an obstacle for northward flowing wind. The GWD enhancement region (Fig. 11b, snapshot for a SSWbox run) is constantly flown around inducing a significant mean anomaly (Fig. 11c, d) with anomalous upwelling in its southern part and downwelling on the northern flank. But, the GWD region (obstacle) creates also a lee wave like pattern with oscillating anomalies in the upper stratosphere and in the SH. Considering a time mean, these anomalies are small and not significant, but, at particular time steps, the magnitude of the anomalies is comparable regardless of the BDC branch. Supporting information is given in Animation 3 in the Supplement, which presents the time evolution of the zonal mean residual circulation associated mass flux for the 10box simulation (on the left) together with its anomaly (on the right). One can see here the global nature of the response and gain insight into how quickly the residual circulation gets affected by the NH anomalous forcing. After few time-steps, the response is constituted by a constant anomaly corresponding roughly to an accelerated shallow BDC branch sloping down from approx. 30km at the North Pole to the lowest analyzed levels at the equator. Except for this region, the entire domain is dominated by anomalies seemingly descending downward from the mesosphere associated with the obstacle analogy.

The zonal structure of the induced flow, and possible consequences of the GW hotspot for the longitudinal variability of the BDC were studied by means of 3D residual circulation analysis according to Kinoshita and Sato (2013). 5-day running averaging was performed. Šácha et al. (2015) pointed out unusually high temperatures in the EA/NP region at 30 hPa in winter and concluded that there could be an enhanced downwelling above the EA/NP region penetrating to lower levels than elsewhere. This is in agreement with Fig. 3 in Demirhan Bari et al. (2013). Supporting results highlighting the importance of future research in this region are given in the supplement. In Fig. 1S in the supplement we present a thirty-year average January MSR total ozone column field with a total ozone column maximum located in the EA/NP region. In Fig. 2S in the supplement, longitudinal cross-sections of MIPAS CH_4 volume mixing ratios show a peak of subsidence around 15 km in the EA/NP region (at 140°E) and the interesting massive upwelling branch east of it.

To evaluate the possible role of the GW activity in the longitudinal variability of the BDC, we present longitudinal cross-sections of the reference 3D vertical residual velocity and Box0.1 anomalies going from the northern to southern part of the artificial GWD (Fig. 12). From longitudinal cross-sections of the reference vertical residual velocity (left side of Fig. 12), we see that MUAM vertical residual velocity field is dominated by a wave-2 pattern, with the maximum subsidence branch penetrating to the lower stratosphere in the EA/NP region and with an abrupt switch to upwelling on the east. Ridges

Petr Šácha 13.10.16 13:04
Deleted: approximately …bove the ... [76]

Petr Šácha 13.10.16 13:13
Deleted: occasionally reach a few percent. This, together with the previously unexpected fact of a weak upper branch BDC response to the artificial GWD can be rather explained by the effect of a monthly averaging than due to the locality of the residual circulation response to the artificial GWD (see Animation 4 in the Supplement). At particular time steps the magnitude of the anomalies is comparable regardless on the BDC branch, but for the deep BDC branch the anomalies oscillate.
In Fig. 8 we can see a significant total ozone column maximum corresponding to the EA/NP region. When presenting total column ozone one has to have in mind the westward shift of the subsidence area with height (see Fig. 9, upper row) and take into account the climatological height profile of ozone concentrations. Mean January zonal cross-sections of MUAM vertical residual velocity for the reference simulation (Fig. 9, upper row) give insight into the zonal structure of the residual circulation. A good correspondence between the location of the maximal subsidence branch in Fig. 9 and the location of the total ozone column maximum (having the above discussed prerequisites in mind), shows that the enhanced downwelling pattern in the EA/NP region is well captured in MUAM.
…

Petr Šácha 13.10.16 21:41
Formatted: Widow/Orphan control, Adjust space between Latin and Asian text, Adjust space between Asian text and numbers

Petr Šácha 19.10.16 10:39
Deleted: i… performed. The averagi ... [77]

Petr Šácha 13.10.16 21:54
Deleted: In Fig. 8 we can see a significant column maximum corresponding to the EA/NP region. When presenting total column ozone one has to have in mind the westward shift of the subsidence area with height (see Fig. 9, upper row) and take into account the climatological height profile of ozone concentrations. Mean January zonal cross-sections of MUAM vertical residual velocity for the reference simulation (Fig. 9, upper row) give insight into the zonal structure of the residual circulation. A good correspondence between the location of the maximal subsidence branch in Fig. 9 and the location of the total ozone column maximum (having the above discussed prerequisites in mind ... [78]

Petr Šácha 19.10.16 11:10
Formatted: English (AUS)

Petr Šácha 15.10.16 13:57
Deleted: in …ig. 1…2)0… The ano ... [79]

Petr Šácha 19.10.16 11:10
Formatted: English (AUS)

and troughs of the wave show a characteristic westward tilt with height.

Šácha et al. (2015) hypothesized that the collocation of the EA/NP GW hotspot and the enhanced BDC branch can be partly a consequence of the circulation induced by the GW breaking. But the results are rather contradictory. In agreement with the zonal mean residual circulation analysis, we can see that in the southern part of the area (Fig. 12f), the GWD induces predominantly anomalous upward flow. Anomalous subsidence strengthens when going further northward (Fig. 12b, d). In line with the obstacle analogy, we observe subsidence in the eastern part of the GWD region only, while anomalous upward flow dominates the western part of the GWD region, and then again eastward and slightly above the anomalous subsidence area. Similar structure of an Eulerian mean vertical velocity field has been found by Shaw and Boos (2012) as a response to an artificial torque placed in the troposphere around 30°N. These results show that GWs can contribute to longitudinal variations in the BDC and not only the downwelling, but also upwelling patterns may be related with GWs.

The magnitude of the vertical residual velocity anomalies maximizes around 2% of the reference value for the Box0.1 simulation (Fig. 12b, d, f). For the 10box simulation (Fig. 3S in the Supplement) the distribution of upwelling and subsidence is identical and the magnitude reaches 30% locally. Physically, such an anomalous pattern can be explained by considering the dominant background horizontal north-eastward wind together with the previously mentioned small obstacle analogy, with induced upward flow upwind and downward flow downwind from the GWD box. However, for the SSWbox simulation we can observe a completely different distribution variable with time, with subsidence dominating directly above the GWD area in the later stages of the simulation (Animation 4 in the Supplement). When the artificial GWD is strong enough to induce significant dynamical changes (SSW simulations) the anomalies cannot be directly explained as being GW induced because also the dynamical state of the atmosphere changes (e.g. the anticyclonic evolution in Animation 1a). Therefore, the explanation of residual vertical wind cross-section patterns for both SSW simulations is much more complicated and requires future research allowing at least the GWD enhancement to reflect the changing background conditions.

4. Discussion and conclusions

We will begin this section by giving a brief summary of results. Then, we will discuss limits of our results stemming from the construction of the sensitivity simulations and afterwards, we will give some conclusions for different research topics in the middle atmosphere.

In this paper, we presented results of a set of sensitivity simulation to find out the possible role of a localized GW hotspot and also, generally, to demonstrate the influence of spatial distribution of GWD on the middle atmospheric dynamics. The focus was on a mean response to a steady GWD perturbation injected into climatological January condition. Except for the strongest GWD enhancement (SSW simulations; Fig.3), all simulations (Table 1) have reached a quasi steady state approximately 7 days after the GWD enhancement (Fig. 3). The average across this state was considered as a mean response later in the text. Section 3.1 was concerned with a mean geopotential response at the 6.25 hPa level (Fig. 5). Mean anomalies (differences with reference) were found to be largest in the polar region and

Petr Šácha 14.10.16 11:46
Formatted: Font:(Default) +Theme Body

Petr Šácha 14.10.16 11:42
Deleted: …ácha et al. (2015) hypot ... [80]

Petr Šácha 16.10.16 15:12
Deleted: …he magnitude of the ver ... [81]

larger for the box GWD enhancements (both globally and locally) than for the corresponding ring enhancements. The important role of a purely constraint (from observations) meridional GWD component, especially for the polar vortex response, was highlighted. Most importantly, for simulations with the strongest GWD enhancement (SSWbox and SSWzon; Table 1), we observed different types of polar vortex events, namely a vortex split in response to the ring GWD enhancement and a vortex displacement for a localized forcing (Fig. 6).

In section 3.2 we studied the influence of the artificial GWD and of its distribution on the PW activity. We have found (Fig. 7) mean E-P flux convergence anomaly centered at the equatorward flank of the GWD enhancement area and an anomalous convergence in a broad area around 60°N in response to the artificial GWD. The anomalies are bigger for the box enhancements and in the box simulations we have also identified anomalous, predominantly horizontal PW propagation indicative of in-situ PW generation. This is further supported by the results of FT analysis of the geopotential anomalies (Fig.9), where, for the box simulations we have found especially the wave-1 and also wave-3 mean amplitude anomalously enhanced. Also, the short-term response (Fig. 10) showed the origin of the enhanced amplitudes to be in the GWD area.

Section 3.3 has been concerned with a residual circulation response. It was shown that there are significant differences in a zonal mean residual circulation between different distributions of the same zonal mean GWD (Fig. 11). A butterfly like pattern in the box-ring differences was identified centered at approximately 45°N (the center of the GWD region), with a stronger/weaker subsidence north/south of the enhancement region in the box simulations between 20 and 30 km log-pressure height. Evidence was given that the artificial GWD in our model acts like a small obstacle for the flow, which was further supported by the 3D residual circulation analysis (Fig. 12). We have found downwelling to the northeast (downwind) and upwelling to the southwest (upwind) of the GWD box showing that GWs can contribute to longitudinal variations in the BDC.

The biggest limit of our analysis is naturally the artificiality of our GWD enhancement. The GWD enhancement introduces an additional artificial constant momentum sink in the model. The concept of the artificial GWD enhancement leaves us also no chance to reflect any feedback between GWs and background conditions (changes in background winds, evolving PW field, etc.). Therefore, for example, our simulation of a vortex displacement differs from reality by not reflecting the background changes, as the GWs are known to be significantly filtered during SSWs (e.g. Holton, 1983; Limpasuvan et al., 2012). Considering the intermittent nature of GWs (e.g. Hertzog et al., 2012; Wright et al., 2013), another inaccuracy of our sensitivity simulation set-ups arises from the constancy of the artificial GWD. In particular in the EA/NP region, where we expect mountain wave forcing to be prominent in January, variations of more than an order of magnitude from day to day are to be expected (Schroeder et al., 2009). A multiple (during a month) pulse like injection of the artificial GWD would be arguably more realistic, but on the expense of absense of any steady response during the whole simulation. It is also a question, what is a more realistic illustration of the GW effect on the atmosphere, a sudden GWD injection or smooth increase and decrease with e.g. a 10-day e-folding time to minimize the initial adjustment noise as proposed by Holton (1983)? Also the spatial

Petr Šácha 16.10.16 16:32
Deleted: discussing the discrepancy of the subsidence pattern between different GWD set-ups (Box0.1 and SSW simulations). These are probably due to the induced dynamical changes in the model state of the atmosphere in the SSW simulation. Also, a contrasting effect of the different GWD components and their different ratios may to some extent determine the induced residual circulation pattern, e.g. the heating induced by GW breaking related mixing - positive in our case - induces a positive geopotential anomaly locally, while the meridional component of GWD is connected with a negative anomaly (See Fig. 3). ... [82]

Petr Šácha 17.10.16 10:10
Deleted: t

Petr Šácha 17.10.16 11:04
Formatted: Space After: 6 pt, Widow/Orphan control, Adjust space between Latin and Asian text, Adjust space between Asian text and numbers

Petr Šácha 17.10.16 10:11
Deleted:

Petr Šácha 17.10.16 10:11
Deleted: when comparison is made with observations

Petr Šácha 17.10.16 10:11
Deleted: Our

Petr Šácha 17.10.16 10:12
Deleted: , like the previously discussed

Petr Šácha 17.10.16 10:13
Deleted: induced vertical movements

Petr Šácha 17.10.16 10:12
Deleted: or the

Petr Šácha 17.10.16 10:16
Deleted:

Petr Šácha 17.10.16 10:14
Deleted: is not very reliable

Petr Šácha 16.10.16 22:46
Deleted: Also, the injection of the artificial GWD is responsible for creation of inertia GWs. In our results we always pointed out when a particular feature was caused by inertia GWs, because they are a result of our sensitivity simulation set-up. Nevertheless, we believe that it is interesting to describe ... [83]

Petr Šácha 17.10.16 13:00
Deleted:

Petr Šácha 17.10.16 10:17
Deleted: of massive inertia GW occurrence

Petr Šácha 19.10.16 21:00
Deleted:

Petr Šácha 19.10.16 20:58
Deleted:

distribution of our artificial GWD is highly idealized (in both the horizontal and the vertical). We must note that we compare two "extreme" GWD longitudinal distributions only. It is also very likely that the sharp boundaries of the GWD enhancement in the 10box/zon and SSWbox/zon simulation are influencing some minor patterns of the response (e.g. the lee wave pattern in Fig. 10b).

In future work it is therefore necessary to take into account more realistic GWD distributions to address e.g. the efficiency of PW creation. For example, it is possible that a configuration of GWD taking into account the EA/NP and e.g. the Greenland GW activity hotspot would favour enhanced wave-2 instead of wave-1 activity, and for comparison a chessboard-like or random distribution of GWD would possibly be more appropriate for comparison. Generally, the fact that the PW activity depends on the longitudinal GWD distribution (Fig. 7) suggests that the rate of compensation between resolved and unresolved drag (Cohen et al. 2013, 2014) can be variable in dependence on the GWD distribution influencing the efficiency of PW creation.

Another motivation for future research is to concentrate on the position of the GW hotspots relative to the climatological stationary wave location in the stratosphere and to analyze the interaction between the GWD effects and the climatological waves. For example, the EA/NP hotspot lies in the region of the phase transition between a trough and ridge of the climatological wave-1 and our results show (Fig. 8) an anomalous amplification of wave-1 amplitude for a box GWD enhancement in this region. The importance of standing waves for polar vortex strength is well recognized (Watt-Meyer and Kushner, 2015; Yamashita et al., 2015).

In the atmosphere, the most natural, immediate and fastest way for communication of information in the vertical are the GWs (apart from acoustic and acoustic-gravity waves with effects much higher in the atmosphere). We can argue that any change in the troposphere resulting in changes of sourcing, propagation or breaking conditions for GWs will almost immediately influence the distribution of GWD in the stratosphere, with possible effects demonstrated in our paper (in-situ generation of PWs in the lower stratosphere, anomalous vertical movements, etc.). For example, on the interannual scale, the occurrence and strength of the EA/NP GW hotspot can be dependent on the Pacific Decadal Oscillation (PDO) phase and can play a role in the relationship between PDO and SSW occurence frequency (Kren et al., 2015; Woo et al., 2015; Kidston et al., 2015).

There are more conclusions relevant for the SSW research in our results. It is common methodology (see e.g. Albers and Birner (2014) for a review of SSW preconditioning concepts) to estimate e.g. the relative impact of GWs and PWs on polar vortex preconditioning from zonal mean values of zonal forces only. But our results show that the dynamical effect of forcing depends also on its distribution. The impact connected with a localized area connected with a higher value of drag can be much stronger than one would expect from the zonal mean value only. Importantly, we have found that for a sufficiently strong artificial zonal mean zonal force there is a vortex split response to the ring artificial GWD configuration and vortex displacement for a localized forcing. We aim to investigate this in more detail and also for more realistic forcing distributions, but it seems to be clear at this stage that the SSW type may be determined also by the geometry of the forcing, not only by the vortex geometry. On the

Petr Šácha 17.10.16 13:00
Deleted: ... [84]
Petr Šácha 19.10.16 11:26
Deleted:
Petr Šácha 17.10.16 11:48
Deleted:
Petr Šácha 17.10.16 13:03
Formatted: English (US)
Petr Šácha 17.10.16 10:55
Deleted: analyze
Petr Šácha 17.10.16 10:55
Deleted: the role
Petr Šácha 17.10.16 10:55
Deleted: position
Petr Šácha 17.10.16 10:59
Deleted: ,
Petr Šácha 17.10.16 11:00
Deleted: with special focus on the position of
Petr Šácha 17.10.16 11:00
Deleted: transition
Petr Šácha 17.10.16 11:01
Deleted: .
Petr Šácha 17.10.16 10:54
Deleted:
Petr Šácha 17.10.16 11:08
Deleted: (
Petr Šácha 17.10.16 13:04
Deleted: Hypothetically,
Petr Šácha 17.10.16 11:28
Formatted: Font:(Default) Times New Roman
Petr Šácha 17.10.16 11:28
Formatted: Font:(Default) +Theme Body, Czech
Petr Šácha 17.10.16 13:08
Formatted: Space After: 12 pt, No widow/orphan control, Don't adjust space between Latin and Asian text, Don't adjust space between Asian text and numbers
Petr Šácha 17.10.16 11:33
Deleted: sea surface temperature PDO induced anomalies leading to anomalous surface winds (or convection) and consequent anomalous orographic (or convective) GW creation can immediately influence the distribution of GW breaking (not only) in the lower stratosphere with possible in-situ lower stratospheric effects as shown in our results. This does not need to work for the PDO only, a similar mechanism can also be behir ... [85]
Petr Šácha 19.10.16 11:28
Deleted: ,
Petr Šácha 19.10.16 11:29
Deleted: higher

other hand, vortex geometry can to a large extent influence the distribution of the forcing, e.g. spontaneous emission processes connected with the jet (Plougonven and Zhang, 2014).

Blocking connection with SSWs is a well-known correlation (e.g. Andrews et al., 1987; Martius et al., 2009; Nakamura et al., 2014; Albers and Birner, 2014) but the mechanisms standing behind are still rather elusive. The geographical location and evolution of the stationary positive geopotential anomaly with anomalous anticyclonic horizontal winds upstream of the GWD area is a remarkable feature of the atmospheric response to a localized GWD (Fig. 5) suggesting that GWs can be one of the missing mechanisms behind this relationship. This is connected with the important role of the meridional GWD component, especially for the polar vortex response. Interestingly, this feature becomes apparent for the localized enhancement only and has an almost negligible effect in simulations with ring enhancements. To our knowledge, the effect of the meridional component of GWD on the middle atmospheric circulation has not been studied yet. Also, horizontal GW propagation is neglected in most climate model parameterizations (Kalisch et al., 2014). Thus, it is not surprising that there are only few modelling constraints regarding the horizontal propagation directions, although some information is available from ray tracing simulations (Preusse et al., 2009). In most studies based on satellite data, GW propagation directions have not been analysed, because the information needed for such computation (e.g. hodograph analysis) is not available for most of the global observational instruments and their combinations (Wang and Alexander, 2010).

Finally, regarding polar vortex effects, the anomalous PW generation and breaking may be the physical justification for disturbing the vortex in its central levels which was a mechanism hypothesized by Scott and Dritschel (2005). Traditionally, PWs are thought to be generated in the troposphere and propagate up on the polar vortex edge. But, as Scott and Dritschel (2005) pointed out, when wave amplitudes become large and nonlinear effects become important, the notion of upward propagation ceases to be appropriate. Therefore, they considered an option of some in situ disturbance at a given level, with a possible explanation being what we propose - localized GW breaking inducing anomalous PW activity.

Regarding residual circulation, a general conclusion of this paper is that for the same magnitude of an artificial zonal mean zonal force (zonal mean meridional force as well) there are significant differences (depending on the magnitude of the GWD enhancement) in the zonal mean residual circulation between different distributions of this force (localized vs. zonally uniform). Also our results indicate that the distribution of GWD may play a role in zonal asymmetries of the BDC. This is a clear signal that e.g. in the research of future BDC changes from climate models we need to be concerned not merely by the magnitude or latitude-height profile of the zonal mean GWD but also by its zonal distribution. In particular, the models should be able to mimic the main GW activity hotspots. This suggests the need for improvement especially of the nonorographic GW parameterization (though nonorographic GW are usually assumed to have significant effect at higher altitudes than in the vertical range analyzed in this paper), since many global climate models use e.g. a globally uniform gravity wave source function (Geller et al., 2013).

Petr Šácha 19.10.16 11:29
Deleted: side

Petr Šácha 17.10.16 13:15
Formatted: Font:Not Italic

Petr Šácha 17.10.16 13:15
Formatted: Font:Not Italic

Petr Šácha 17.10.16 13:15
Formatted: Font:Not Italic

Petr Šácha 17.10.16 13:15
Formatted: Font:Not Italic

Petr Šácha 17.10.16 13:20
Deleted: ... [86]

Petr Šácha 17.10.16 13:19
Formatted: Font:(Default) Times New Roman, Font color: Auto, English (AUS)

Petr Šácha 19.10.16 11:30
Deleted: z

Petr Šácha 19.10.16 11:31
Deleted: etc.

Petr Šácha 17.10.16 13:26
Formatted: Font color: Custom Color(RGB(28;27;28)), English (US)

Petr Šácha 17.10.16 13:26
Deleted: A

Petr Šácha 17.10.16 13:26
Deleted: and E-P flux divergence

Code availability

MUAM model code is available from the authors upon request.

Data availability

MIPAS CH_4 volume mixing ratio profiles have been provided by Karlsruhe Institute of Technology (KIT), Institute of Meteorology and Climate Research - Atmospheric Trace Gases and Remote Sensing through https://www.imk-asf.kit.edu/english/308.php. MSR total ozone is available through ESA, Tropospheric Emission Monitoring Internet Service (TEMIS) on http://www.temis.nl/protocols/o3field/o3mean_msr2.php. ERA-Interim temperatures and geopotential heights data have been provided by ECMWF through http://www.ecmwf.int/en/research/climate-reanalysis/era-interim.

Acknowledgements

This study was supported by GA CR under grant 16-01562J and by Deutsche Forschungsgemeinschaft under grants JA 836/30-1 and 836/32-1.

References

Albers, J. R., and T. Birner, 2014: Vortex preconditioning due to planetary and gravity waves prior to sudden stratospheric warmings. Journal of the Atmospheric Sciences, 71 (11), 4028–4054, doi:10. 1175/JAS- D- 14- 0026.1.

Alexander, S. P. and Shepherd, M. G.: Planetary wave activity in the polar lower stratosphere, Atmos. Chem. Phys., 10, 707-718, doi:10.5194/acp-10-707-2010, 2010.

Alexander, M. J., & Sato, K. (2015). Gravity Wave Dynamics and Climate: An Update from the SPARC Gravity Wave Activity. Report on the 35th Session of the Joint Scientific Committee of the World Climate Research Programme 29 June–4 July 2014, Heidelberg, Germany, 9.

Alexander MJ, Geller M, McLandress C, Polavarapu S, Preusse P, Sassi F, Sato K, Eckermann S, Ern M, Hertzog A, Kawatani YA, Pulido M, Shaw T, Sigmond M, Vincent R, Watanabe S. 2010. Recent developments in gravity-wave effects in climate models and the global distribution of gravity-wave momentum flux from observations and models. Q. J. R. Meteorol. Soc. **136**: 1103 – 1124. DOI:10.1002/qj.637

Ayarzaguena, B., U. Langematz, and E. Serrano, 2011: Tropo- spheric forcing of the stratosphere: A comparative study of the two different major stratospheric warmings in 2009 and 2010. J. Geophys. Res., 116, D18114, doi:10.1029/2010JD015023.

Brewer, A.W., 1949: Evidence for a world circulation provided by the measurements of helium and water vapor distribution in the stratosphere. Quart. J. Roy. Meteor. Soc., 75, 351–363.

Petr Šácha 26.9.16 16:15
Deleted:

Butchart, N.: The Brewer–Dobson Circulation, Rev. Geophys., 52, 157–184, doi:10.1002/2013RG000448, 2014.

Bühler, O.: Waves and mean flows, Cambridge University Press, 2014.

Calvo, N., Polvani, L. M., & Solomon, S. (2015). On the surface impact of Arctic stratospheric ozone extremes. Environmental Research Letters, 10(9), 094003.

Chandran, A., R. L. Collins, R. R. Garcia, D. R. Marsh, V. L. Harvey, J. Yue, and L. de la Torre (2013), A climatology of elevated stratopause events in the whole atmosphere community climate model, J. Geophys. Res. Atmos., 118, 1234-1246, doi:10.1002/jgrd.50123.

Cohen, N. Y., E. P. Gerber, and O. Bühler, 2013: Compensation between resolved and unresolved wave driving in the strato- sphere: Implications for downward control. J. Atmos. Sci., 70, 3780–3798, doi:10.1175/JAS-D-12-0346.1.

Cohen, N. Y., E. P. Gerber, and O. Bühler, 2014: What drives the Brewer- Dobson circulation? Journal of the Atmospheric sciences, 71, 3837–3855, doi: 10.1175/JAS-D-14-0021.1

Cullens, C. Y., S. L. England, and T. J. Immel (2015), Global responses of gravity waves to planetary waves during stratospheric sudden warming observed by SABER, J. Geophys. Res. Atmos., 120, 12,018–12,026, doi:10.1002/2015JD023966.

Demirhan Bari, D., Gabriel, A., Körnich, H., and Peters, D. W. H.: The effect of zonal asymmetries in the Brewer-Dobson circu- lation on ozone and water vapor distributions in the northern middle atmosphere, J. Geophys. Res.-Atmos., 118, 3447–3466, doi:10.1029/2012JD017709, 2013.

Dobson, G. M. B. (1956). Origin and distribution of the polyatomic molecules in the atmosphere. Proceedings of the Royal Society of London. Series A, Mathematical and Physical Sciences, 236(1205), 187-193.

Dunkerton, T. (1978), On the mean meridional mass motions of the stratosphere and mesosphere, J. Atmos. Sci., 35, 2325–2333.

Dunkerton, T. J., and N. Butchart, 1984: Propagation and selec- tive transmission of internal gravity waves in a sudden warming. J. Atmos. Sci., 41, 1443–1460, doi:10.1175/ 1520-0469(1984)041,1443:PASTOI.2.0.CO;2.

ECMWF (2016), ERA-Interim, http://www.ecmwf.int/en/research/climate-reanalysis/era-interim, downloaded at 15.3.2016.

Petr Šácha 26.9.16 16:14
Formatted: Font:Not Bold, Not Italic, Font color: Auto

Petr Šácha 26.9.16 16:14
Formatted: Font:Not Bold, Not Italic, Font color: Auto

Ern, M., Preusse, P., Gille, J., Hepplewhite, C., Mlynczak, M., Rus- sell, J., and Riese, M.: Implications for atmospheric dynamics de- rived from global observations of gravity wave momentum flux in stratosphere and mesosphere, J. Geophys. Res.-Atmos., 116, D19107, doi:10.1029/2011JD015821, 2011.

France, J. A., and V. L. Harvey (2013), A climatology of the stratopause in WACCM and the zonally asymmetric elevated stratopause, J. Geophys. Res. Atmos., 118, 2241–2254, doi:10.1002/jgrd.50218.

Fritts, D. C. and Alexander, M. J.: Gravity wave dynamics and eff ects in the middle atmosphere, Rev. Geophys., 41, 1003, doi:10.1029/2001RG000106, 2003.

Fröhlich, K., A. Pogoreltsev, and Ch. Jacobi, 2003: Numerical simulation of tides, Rossby and Kelvin waves with the COMMA-LIM model. Adv. Space Res., 32, 863-868, doi:10.1016/S0273-1177(03)00416-2.

Garny, H., T. Birner, H. Bönisch, and F. Bunzel (2014), The effects of mixing on age of air, J. Geophys. Res. Atmos., 119, 7015–7034, doi:10.1002/2013JD021417.

Geller, M. A., Alexander, M. J., Love, P. T., Bacmeister, J., Ern, M., Hertzog, A., Manzini, E., Preusse, P., Sato, K., Scaife, A. A., and Zhou, T.: A comparison between gravity wave momentum fluxes in observations and climate models, J. Climate, 26, 6383–6405, doi:10.1175/JCLI-D-12-00545.1, 2013.

Gerber, E. P., A. Butler, N. Calvo, A. Charlton-Perez, M. Giorgetta, E. Manzini, J. Perlwitz, L. M. Polvani, F. Sassi, A. A. Scaife, T. A. Shaw, S.-W. Son, and S. Watanabe, 2012: Assessing and understanding the impact of stratospheric dynamics and variability on the Earth system, B. Amer. Meteorol. Soc., 93, 845–859.

Hardiman, S. C. and P. H. Haynes, 2008: Dynamical sensitivity of the stratospheric circulation and downward influence of upper level perturbations, J. Geophys. Res., 113, D23 103, doi:10.1029/2008JD010168.

Hardiman, S. C., Andrews, D. G., White, A. A., Butchart, N., and Edmond, I.: Using Different Formulations of the1065 Transformed Eulerian Mean Equations and EliassenPalm Diagnostics in General Circulation Models, J. Atmos. Sci., 67, 1983–1995, doi:doi:10.1175/2010JAS3355.1, http://dx.doi.org/ 10.1175/2010JAS3355.1, 2010.

Haynes, P.: Stratospheric Dynamics, Annu. Rev. Fluid Mech., 37, 263–293, doi:10.1146/annurev.fluid.37.061903.175710, 2005.

Haynes, P., McIntyre, M., Shepherd, T., Marks, C., and Shine, K. P.: On the "downward control" of extratropical diabatic circulations by eddy-induced mean zonal forces, J. Atmos. Sci., 48, 651–678, 1991.

He, C., Zhou, T., Lin, A., Wu, B., Gu, D., Li, C., & Zheng, B. (2015). Enhanced or Weakened Western North Pacific Subtropical High under Global Warming?. Scientific reports, 5.

Hertzog, A., Alexander, M. J., and Plougonven, R.: On the intermittency of gravity wave momentum flux in the stratosphere, J. Atmos. Sci., 69, 3433–3448, 2012.

Hoffmann, P., W. Singer, D. Keuer, W. K. Hocking, M. Kunze, and Y. Murayama (2007), Latitudinal and longitudinal variability of mesospheric winds and temperatures during stratospheric warming events, J. Atmos. Sol. Terr. Phys., **69**, 2355–2366.

Holton, J. R., The influence of gravity wave breaking on the general circulation of the middle atmosphere, J. Atmos. Sci., 40, 2497–2507, 1983.

Holton, J. R., 1984: The generation of mesospheric planetary waves by zonally asymmetric gravity wave breaking. J. Atmos. Sci., 41, 3427–3430, doi:10.1175/1520-0469(1984)041,3427: TGOMPW.2.0.CO;2.

Jacobi, Ch., K. Fröhlich, and A. Pogoreltsev, 2006: Quasi two-day-wave modulation of gravity wave flux and consequences for the planetary wave propagation in a simple circulation model, J. Atmos. Sol.-Terr. Phys., 68, 283-292, doi:10.1016/j.jastp.2005.01.017.

Jacobi, Ch., F. Lilienthal, C. Geißler, and A. Krug, 2015: Long-term variability of mid-latitude mesosphere-lower thermosphere winds over Collm (51°N, 13°E), J. Atmos. Sol.-Terr. Phys., 136, B, 174–186, doi:10.1016/j.jastp.2015.05.006.

Kalisch, S., P. Preusse, M. Ern, S. D. Eckermann, and M. Riese, 2014: Differences in gravity wave drag between realistic oblique and assumed vertical propagation, J. Geophys. Res. Atmos., 119, 10,081–10,099, doi:10.1002/2014JD021779.

Kidston, J., A. A. Scaife, S. C. Hardiman, D. M. Mitchell, N. Butchart, M. P. Baldwin, and L. J. Gray (2015), Stratospheric influence on tropospheric jet streams, storm tracks and surface weather, Nat. Geosci., 8, 433–440, doi:10.1038/ngeo2424.

Petr Šácha 19.10.16 21:10
Deleted: ... [87]

KIT (2016), Access to IMK/IAA generated MIPAS/Envisat data, https://www.imk-asf.kit.edu/english/308.php, downloaded at 01.02.2016.

Kinoshita, T., & Sato, K. (2013). A formulation of three-dimensional residual mean flow applicable both to inertia–gravity waves and to Rossby waves. Journal of the Atmospheric Sciences, 70(6), 1577-1602.

Kren, A. C., Marsh, D. R., Smith, A. K., & Pilewskie, P. (2015). Wintertime Northern Hemisphere response in the Stratosphere to the Pacific Decadal Oscillation using the Whole Atmosphere Community Climate Model. Journal of Climate, (2015).

Kuroda, Y., 2008: Effect of stratospheric sudden warming and vortex intensification on the tropospheric climate. J. Geophys. Res., **113**, D15110, doi:10.1029/2007JD009550.

Kuttippurath, J. and Nikulin, G.: A comparative study of the major sudden stratospheric warmings in the Arctic winters 2003/2004–2009/2010, Atmos. Chem. Phys., 12, 8115-8129, doi:10.5194/acp-12-8115-2012, 2012.

Lawrence, B.N. (1997) The Effect of Parameterized Gravity Wave Drag on Simulations of the Middle Atmosphere During Northern Winter 1991/1992-General Evolution. NATO ASI SERIES I GLOBAL ENVIRONMENTAL CHANGE, 50. pp. 291-308.

Lehtonen, I., and A. Y. Karpechko (2016), Observed and modeled tropospheric cold anomalies associated with sudden stratospheric warmings, J. Geophys. Res. Atmos., 121, 1591–1610, doi:10.1002/2015JD023860.

Lieberman, R. S., D. M. Riggin, and D. E. Siskind, 2013: Stationary waves in the wintertime mesosphere: Evidence for gravity wave filtering by stratospheric planetary waves, J. Geophys. Res., 118, 3139–3149, doi:10.1002/jgrd.50319.

Limpasuvan, V., Richter, J. H., Orsolini, Y. J., Stordal, F., and Kvissel, O.-K.: The roles of planetary and gravity waves during a major stratospheric sudden warming as characterized in WACCM, J. Atmos. Sol.-Terr. Phys., 78–79, 84–98, 2012.

Lindzen, R.S., 1981. Turbulence and stress owing to gravity wave and tidal breakdown. Journal of Geophysical Research 86, 9709–9714.

Manney, G. L., M. J. Schwartz, K. Krüger, M. L. Santee, S. Pawson, J. N. Lee, W. H. Daffer, R. A. Fuller, and N. J. Livesey, 2009: Aura Microwave Limb Sounder observations of dynamics and transport during the record-breaking 2009 Arctic stratospheric major warming, Geophys. Res. Lett., 36, L12815, doi:10.1029/2009GL038586.

Petr Šácha 19.10.16 21:10
Deleted: ... [88]

Petr Šácha 17.10.16 13:35
Deleted: Liu, H.-L., Hagan, M., and Roble, R.: Local mean state changes due to gravity wave breaking modulated by the diurnal tide, J. Geophys. Res., 105, 12381–12396, ... [89]

Manzini, E., et al. (2014), Northern winter climate change: Assessment of uncertainty in CMIP5 projections related to stratosphere-troposphere coupling, J. Geophys. Res. Atmos., 119, 7979–7998, doi:10.1002/2013JD021403.

Martius, O., L. Polvani, and H. Davies, 2009: Blocking precursors to stratospheric sudden warming events. Geophys. Res. Lett., 36, L14806, doi:10.1029/2009GL038776.

Matsuno, T., 1966. Numerical integration of the primitive equations by a simulated backward difference method. Journal of Meteorological Society of Japan 44, 76–84.

McFarlane, N.A., The effect of orographically excited gravity wave drag on the general circulation of the lower stratosphere and troposphere, J. Atmos. Sci., 44, 1775-1800, 1987.

McLandress, C., S. Polavarapu, and S. R. Beagley, 2012: Is missing orographic gravity wave drag near 608S the cause of the stratospheric zonal wind biases in chemistry climate models? J. Atmos. Sci., 69, 802–818.

Nakamura, H., Nishii, K., Wang, L., Orsolini, Y. J., & Takaya, K., 2014: Cold-air outbreaks over East Asia associated with blocking highs: Mechanisms and their interaction with the polar stratosphere. *Dynamics and Predictability of Large-Scale High-Impact Weather and Climate Events*, 2.

Nishii, K., H. Nakamura, and T. Miyasaka, 2009: Modulations in the planetary wave field induced by upward propagating Rossby wave packets prior to stratospheric sudden warming events: A case study, Q. J. Roy. Meteor. Soc., 135, 39-52.

Oberheide, J., H.-L. Liu, O. Gusev, and D. Offermann, 2006: Mesospheric surf zone and temperature inversion layers in early November 1994, J. Atmos. Sol.-Terr. Phys., 68, 1752–1763.

Pawson, S. (1997). Effects of gravity wave drag in the Berlin troposphere-stratosphere-mesosphere GCM. In Gravity Wave Processes (pp. 327-336). Springer Berlin Heidelberg.

Plieninger, J., von Clarmann, T., Stiller, G. P., Grabowski, U., Glatthor, N., Kellmann, S., Linden, A., Haenel, F., Kiefer, M., Höpfner, M., Laeng, A., and Lossow, S.: Methane and nitrous oxide retrievals from MIPAS-ENVISAT, Atmos. Meas. Tech., 8, 4657-4670, doi:10.5194/amt-8-4657-2015, 2015.

Plougonven, R. and Zhang, F.: Internal gravity waves from atmospheric jets and fronts, Rev. Geophys., 52, 33–76, doi:10.1002/2012RG000419, 2014.

Pogoreltsev, A.I., A.A. Vlasov. K. Fröhlich, and Ch. Jacobi, 2007: Planetary waves in coupling the lower and upper atmosphere, J. Atmos. Sol.-Terr. Phys., 69, 2083-2101, doi:10.1016/j.jastp.2007.05.014.

Preusse, P., S. D. Eckermann, M. Ern, J. Oberheide, R. H. Picard, R. G. Roble, M. Riese, J. M. Russell III, and M. G. Mlynczak, 2009: Global ray tracing simulations of the SABER gravity wave climatology, J. Geophys. Res., 114, D08126, doi:10.1029/2008JD011214

Ratnam, M.V., T. Tsuda, Ch. Jacobi, and Y. Aoyama, 2004a: Enhancement of gravity wave activity observed during a major Southern Hemisphere stratospheric warming by CHAMP/GPS mea surements. Geophys. Res. Lett., 31, L16101, doi:10.1029/2004GL019789.

Richter, J. H., Sassi, F., & Garcia, R. R. (2010). Toward a physically based gravity wave source parameterization in a general circulation model. Journal of the Atmospheric Sciences, 67(1), 136-156.

Sandu, I., P. Bechtold, A. Beljaars, A. Bozzo, F. Pithan, T. G. Shepherd, and A. Zadra (2016), Impacts of parameterized orographic drag on the Northern Hemisphere winter circulation, J. Adv. Model. Earth Syst., 7, doi:10.1002/2015MS000564.

Schroeder, S., Preusse, P., Ern, M., and Riese, M.: Gravity waves resolved in ECMWF and measured by SABER, Geophys. Res. Lett., 36, L10805, doi:10.1029/2008GL037054, 2009.

Scott, R. K., and D. G. Dritschel. 2005: Downward Wave Propagation on the Polar Vortex. J. Atmos. Sci., **62**, 3382-3395.

Seviour, W. J. M., L. J. Gray, and D. M. Mitchell (2016), Stratospheric polar vortex splits and displacements in the high-top CMIP5 climate models, J. Geophys. Res. Atmos., 121, 1400–1413, doi:10.1002/2015JD024178.

Shaw, T. A., and W. R. Boos, 2012: The tropospheric response to tropical and subtrop- ical zonally-asymmetric torques: Analytical and idealized numerical model results. J. Atmos. Sci., 69, 214-234.

Siskind, D. E., S. D. Eckermann, J. P. McCormack, L. Coy, K. W. Hoppel, and N. L. Baker (2010), Case studies of the mesospheric response to recent minor, major, and extended stratospheric warmings, J. Geophys. Res., 115, D00N03, doi:10.1029/2010JD014114.

Smith, A. K.: The origin of stationary planetary waves in the upper mesosphere, J. Atmos. Sci., 60, 3033–3041, 2003.

Smith, A. K.: Global dynamics of the MLT, Surv. Geophys., 33, 1177–1230, doi:10.1007/s10712-012-9196-9, 2012.

Šácha, P., Foelsche, U., and Pišoft, P.: Analysis of internal gravity waves with GPS RO density profiles, Atmos. Meas. Tech., 7, 4123-4132, doi:10.5194/amt-7-4123-2014, 2014.

Petr Šácha 20.10.16 13:55
Deleted:

Šácha, P., Kuchař, A., Jacobi, C., and Pišoft, P.: Enhanced internal gravity wave activity and breaking over the northeastern Pacific–eastern Asian region, Atmos. Chem. Phys., 15, 13097-13112, doi:10.5194/acp-15-13097-2015, 2015.

TEMIS, Tropospheric Emission Monitoring Internet Service (2016), Monthly mean ozone from the multi-sensor reanalysis (MSR), http://www.temis.nl/protocols/o3field/o3mean_msr.php, downloaded at 10.03.2016.

van der A, R. J., Allaart, M. A. F., and Eskes, H. J.: Extended and refined multi sensor reanalysis of total ozone for the period 1970\u20132012, Atmos. Meas. Tech., 8, 3021-3035, doi:10.5194/amt-8-3021-2015, 2015.

von Clarmann, T., Höpfner, M., Kellmann, S., Linden, A., Chauhan, S., Funke, B., Grabowski, U., Glatthor, N., Kiefer, M., Schieferdecker, T., Stiller, G. P., and Versick, S.: Retrieval of temperature, H2O, O3, HNO3, CH4, N2O, ClONO2 and ClO from MIPAS reduced resolution nominal mode limb emission measurements, Atmos. Meas. Tech., 2, 159-175, doi:10.5194/amt-2-159-2009, 2009.

Walterscheid, R. L. "Inertio-gravity wave induced accelerations of mean flow having an imposed periodic component: Implications for tidal observations in the meteor region." Journal of Geophysical Research: Oceans 86.C10 (1981): 9698-9706.

Wang, L. and M. Alexander, 2010: Global estimates of gravity wave parameters from GPS radio occultation temperature data, J. Geophys. Res., 115, D21122, doi:10.1029/2010JD013860.

Watt-Meyer, O., & Kushner, P. J. (2015). The Role of Standing Waves in Driving Persistent Anomalies of Upward Wave Activity Flux. Journal of Climate, 28(24), 9941-9954.

Woo, S.-H., M.-K. Sung, S.-W. Son, and J.-S. Kug, 2015: Connection between weak stratospheric vortex events and the Pacific Decadal Oscillation. Climate Dynamics, 1-12, doi:10.1007/s00382-015-2551-z.

Wright, C. J., Osprey, S. M., and Gille, J. C.: Global observations of gravity wave intermittency and its impact on the observed mo- mentum flux morphology, J. Geophys. Res.-Atmos., 118, 10980– 10993, doi:10.1002/jgrd.50869, 2013.

Yamashita, C., H.-L. Liu, and X. Chu (2010), Gravity wave variations during the 2009 stratospheric sudden warming as revealed by ECMWF-T799 and observations, Geophys. Res. Lett., 37, L22806, doi:10.1029/2010GL045437.

Yamashita, Y., Akiyoshi, H., Shepherd, T. G., & Takahashi, M., 2015: The Combined Influences of Westerly Phase of the Quasi-Biennial Oscillation and 11-year Solar Maximum Conditions on the Northern Hemisphere Extratropical Winter Circulation. *気象集誌. 第 2 輯*, *93*(6), 629-644, doi:10.2151/jmsj.2015-054.

Petr Šácha 13.10.16 14:09
Deleted: ... [90]

Name	Distribution of the artificial GWD	Artificial gcu per gridpoint of the artificial area (m/s/d)	Zonal mean gcu in the altitude of artificial GWD (m/s/d)	Artificial gcv per gridpoint of the artificial area (m/s/d)	Zonal mean gcv (m/s/d)	Artificial gt per gridpoint of the artificial area (K/d)
Ref	~	~	*0.011*	~	*-0.001*	~
Box0.5	*box*	*-0.5*	*-0.073*	*-0.5*	*-0.085*	*0.05*
Zon0.5	*ring*	*-0.073*	*-0.073*	*-0.085*	*-0.085*	*0.05*
Box0.1pos	*box*	*-0.5*	*-0.073*	*0.1*	*0.018*	*0.05*
Zon0.1pos	*ring*	*-0.073*	*-0.073*	*0.018*	*0.018*	*0.05*
Box0.1	*box*	*-0.5*	*-0.073*	*-0.1*	*-0.016*	*0.05*
Zon0.1	*ring*	*-0.073*	*-0.073*	*-0.016*	*-0.016*	*0.05*
Box0.1gcu	*box*	*-0.5*	*-0.073*	~	*-0.001*	~
Box0.1gcv	*box*	~	*0.011*	*-0.1*	*-0.016*	~
Box0.1gt	*box*	~	*0.011*	~	*-0.001*	*0.05*
10box	*box*	*-10*	*-1.706*	*-0.1*	*-0.016*	*0.05*
10zon	*ring*	*-1.706*	*-1.706*	*-0.016*	*-0.016*	*0.05*
SSWbox	*box*	*-70*	*-12.018*	*-0.1*	*-0.016*	*0.05*
SSWzon	*ring*	*-12.018*	*-12.018*	*-0.016*	*-0.016*	*0.05*

Table 1: Sensitivity simulation names and GWD settings for zonal wind drag (gcu), meridional wind drag (gcv) and heating due to GW (gt) within the box. Note the gcu enhancements are negative because the drag

is westward directed. The distribution describes whether the artificially enhanced GWD is implemented only for certain longitudes (Box) or zonally uniform (Zon). The tilde "~" indicates that values are unchanged w.r.t. the reference simulation. **Note that for a "ring" simulation the gcu values are reduced in such a way that the zonally integrated acceleration is the same as for the corresponding "box" simulation.**

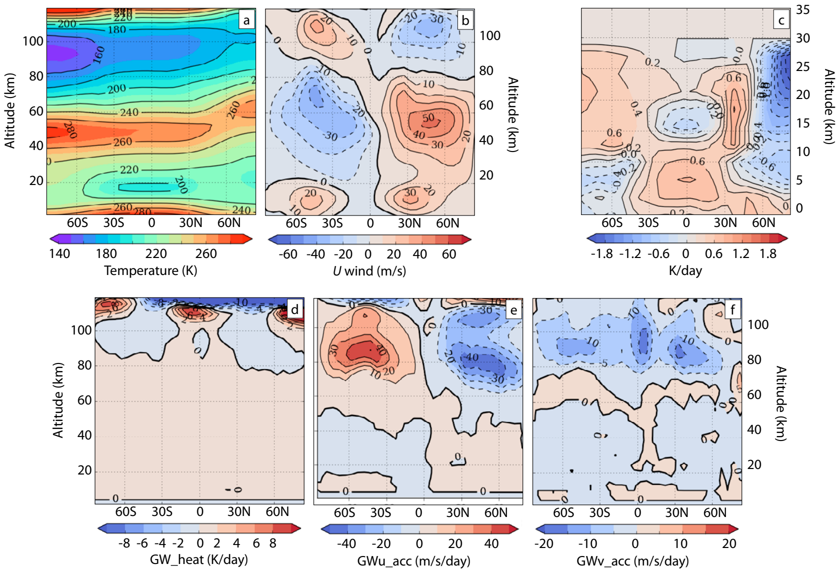

Fig. 1: Mean January zonal means of temperature (a), zonal wind (b), GW induced heating (d) GW induced zonal wind (e) and meridional wind (f) acceleration for the reference simulation. Additionally, January mean zonal mean nudging strength for the strongest GWD injection (SSWbox simulation in Table 1.) is shown (c).

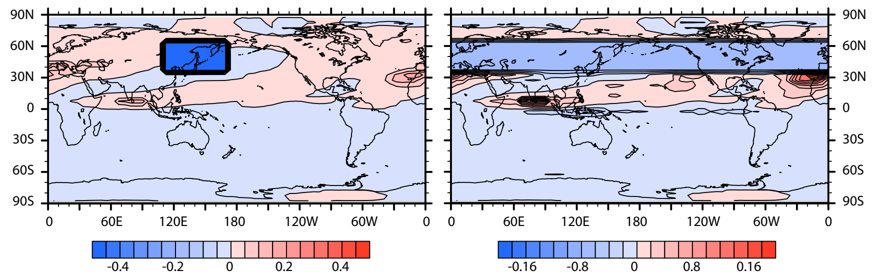

Fig. 2 Two examples of the GWD enhancement horizontal distribution imposed between approximately 20 and 30km of log pressure height. Left panel: box distribution (Box0.1 simulation). Right panel: ring distribution (Zon0.1 simulation). Colors indicate GW induced zonal acceleration [m/s/day].

Unknown
Formatted: Font:(Default) Times New Roman, 8 pt, Bold

Petr Šácha 19.10.16 13:17
Formatted: Font:8 pt, Bold

Petr Šácha 11.10.16 13:46
Deleted: 1

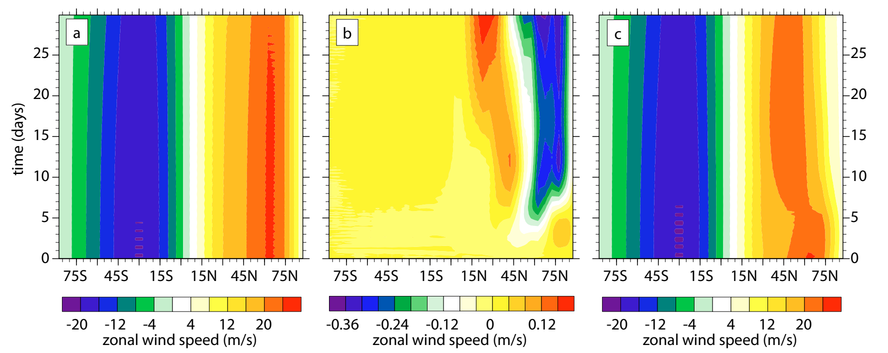

Fig. 3.A Hovmöller diagram of the zonal mean zonal wind for the Ref simulation (a), the zonal mean zonal wind difference with Box0.1 (b) and the zonal mean zonal wind for the 10box simulation at the 6.25 hPa level.

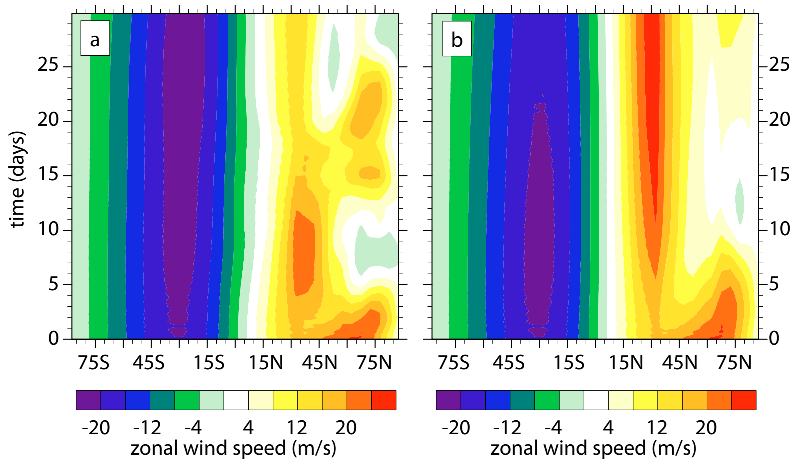

Fig. 4. Hovmöller diagram of the zonal mean zonal wind for the SSWbox simulation (a) and the SSWzon simulation (b) at 6.25hPa.

Unknown
Formatted: Font:8 pt, Font color: Auto

Unknown
Formatted: Font:8 pt, Font color: Auto

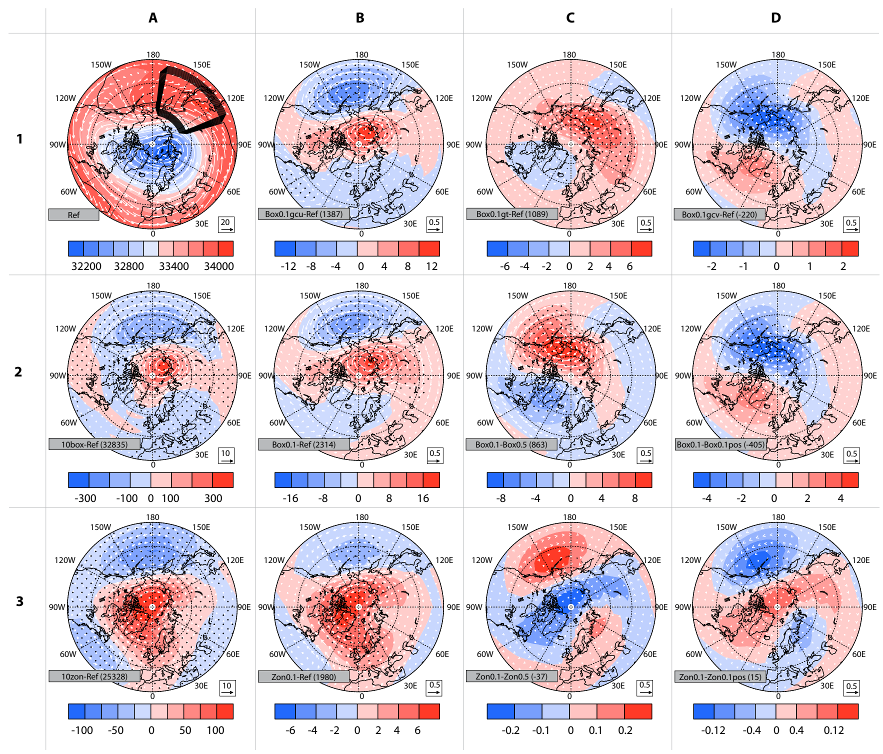

Figure 5: Mean geopotential and horizontal wind vectors at the 13th model level (6.25 hPa) for the reference simulation and differences for the sensitivity simulations with different GWD set-up. From top left (index 1A) to bottom right (index 3D): 1A) reference simulation overlaid with an illustration of the box area, 1B) reference-Box0.1gcu, 1C) reference-Box0.1gt, 1D) reference-Box0.1gcv, 2A) reference-10box, 2B) reference-Box0.1, 2C) Box0.1-Box0.5, 2D) Box0.1-Box0.1pos, 3A) reference-10zon, 3B) reference-Zon0.1, 3C) Zon0.1-Zon0.5 and 3D) Zon0.1-Zon0.1pos. Colors indicate geopotential height [gpm]. Note the different scaling of the respective plots. Arrows refer to horizontal wind [m/s] with unity arrows given below the individual plots. The statistical significance of the mean geopotential differences was computed by a t test and regions with *p* values < 0.05 are stippled. The sum of geopotential difference across the plotted area is given in the legend to each plot.

Petr Šácha 5.10.16 22:03

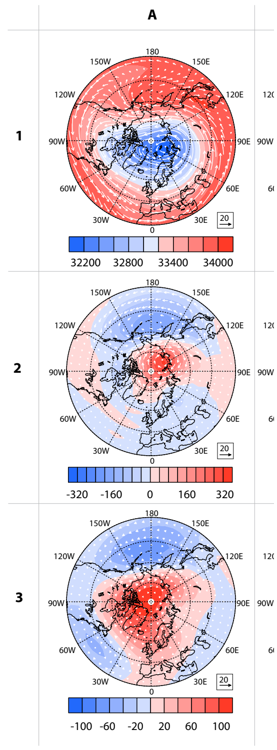

Deleted:

Unknown

Formatted: Font:Not Bold, Font color: Auto

Unknown

Formatted: Font:Not Bold, Font color: Auto

Petr Šácha 5.10.16 21:56

Deleted: 2

Petr Šácha 18.10.16 10:36

Deleted: Monthly

Petr Šácha 18.10.16 10:36

Deleted: m

Petr Šácha 5.10.16 22:02

Formatted: Font:(Default) +Theme Body, Italic, Font color: Auto

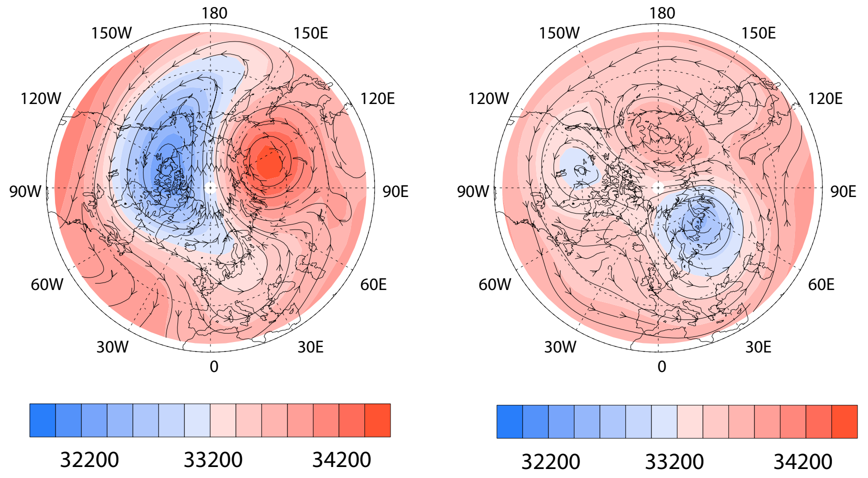

Fig. 6 Geopotential (colors, given in gpm) and horizontal winds (stream lines, given in m/s) for the SSWbox (left) and SSWzon (right) simulation at the 13th model level (6.25 hPa) at 280 hours after the injection.

Petr Šácha 5.10.16 22:05
Deleted: 3

Petr Šácha 5.10.16 11:53
Deleted: 300

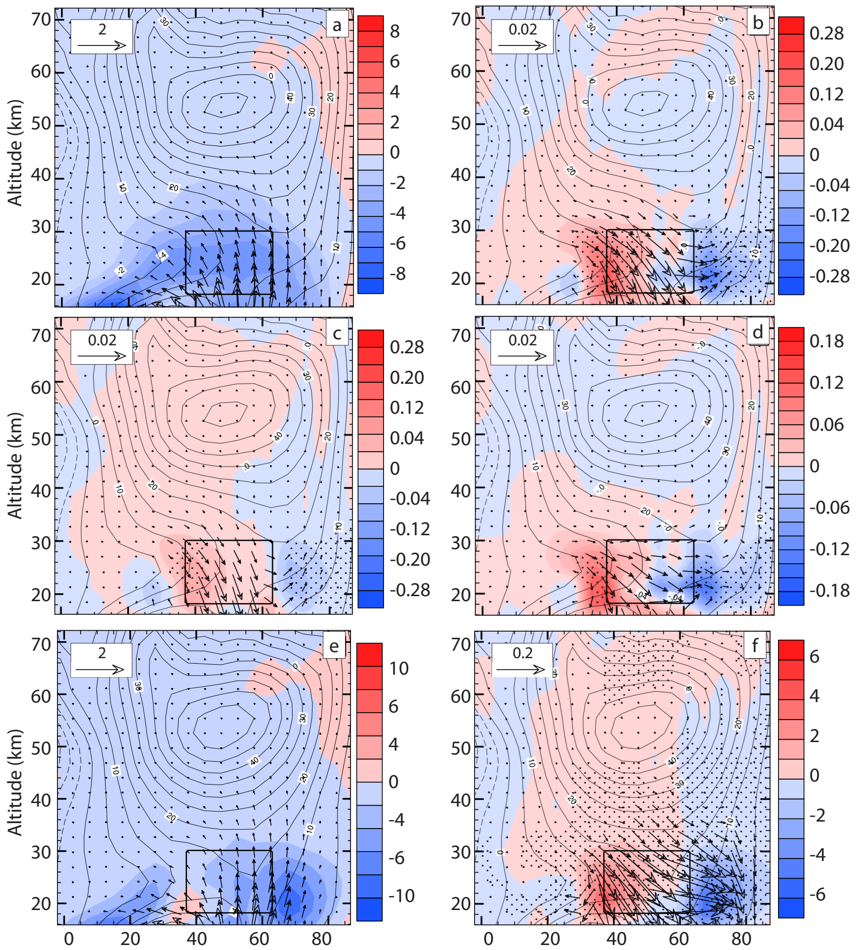

Fig. 7: Mean E-P flux vectors (kgs^{-2}, arrows are scaled according the relative distances of the plot) and its divergence (colors in kg$m^{-1}s^{-2}$) for Box0.1 (a), its anomalies (b), Zon0.1anomalies (c), difference between the Box0.1 and Zon0.1 simulation mean E-P flux and its divergence for 10box (e) and its anomaly (10box-Ref) (f). Note that scales are adjusted for each subfigure, except the plots of anomalies (b,c) sharing the same scaling. In panels (a-f) contours of zonal mean zonal wind from the respective simulations are overlaid with an increment of 10 m/s. All panels are overlaid with selected contour of gravity wave induced zonal acceleration to illustrate the location of artificial GWD. The statistical significance of the mean E-P flux divergence differences was computed by a t test and regions with p values < 0.05 are stippled.

Petr Šácha 11.10.16 14:04

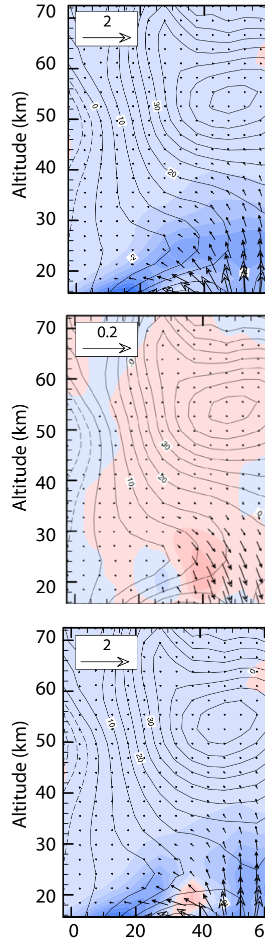

Deleted:

Unknown

Formatted: Font:Not Bold, Font color: Auto

Petr Šácha 11.10.16 14:04

Deleted: 4……. Mean January … ... [91]

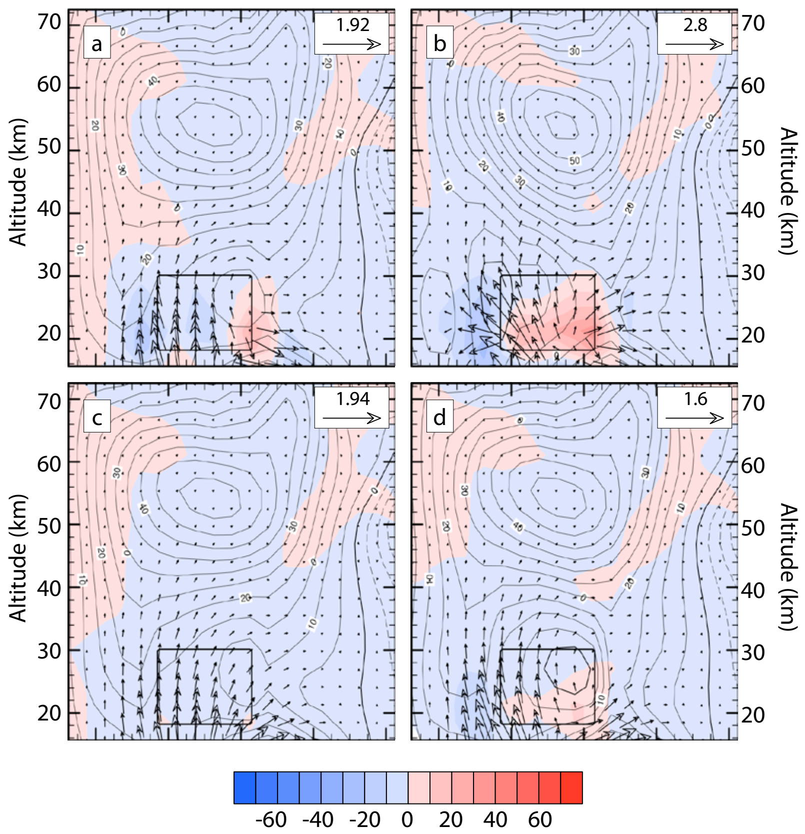

Fig. 8: E-P flux vectors (kgs^{-2}, arrows are scaled according the relative distances of the plot) and its divergence (colors in kgm^{-1}s^{-2}) for the SSWbox simulation at 1 day (a) and 5 days (b) after the GWD injection, for SSWzon 1 day (c) and 5 days (d) after the GWD injection. In all panels contours of zonal mean zonal wind from the respective simulation and time step are overlaid with an increment of 10 m/s. All panels are overlaid with selected contour of gravity wave induced zonal

Unknown
Formatted: Font:(Default) Times New Roman, 8 pt, Bold

Petr Šácha 18.10.16 10:45
Formatted: Left

Petr Šácha 19.10.16 11:36
Formatted: Superscript

Petr Šácha 19.10.16 11:36
Formatted: Superscript

Petr Šácha 19.10.16 11:36
Formatted: Superscript

acceleration to illustrate the location of the artificial GWD.

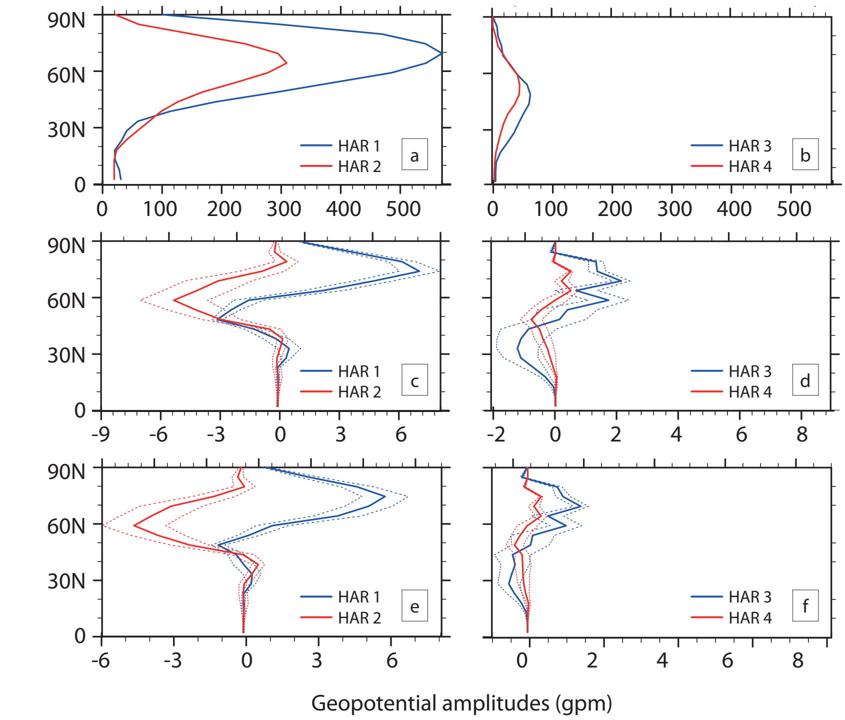

Fig. 9: Mean (7th to 30th day) latitudinal structure of the amplitude of selected harmonics for the Box0.1 simulation. From top left to bottom right: a) harmonics 1 and 2 for Box0.1, b) harmonics 3 and 4 for Box0.1, c) differences of a) from the reference simulation, d) differences of b) from reference simulation, e) differences of a) from Zon0.1, f) differences of b) from Zon0.1. At approx. 35 km log-pressure height. Units are given in [gpm]. Dotted lines show the standard deviation differences.

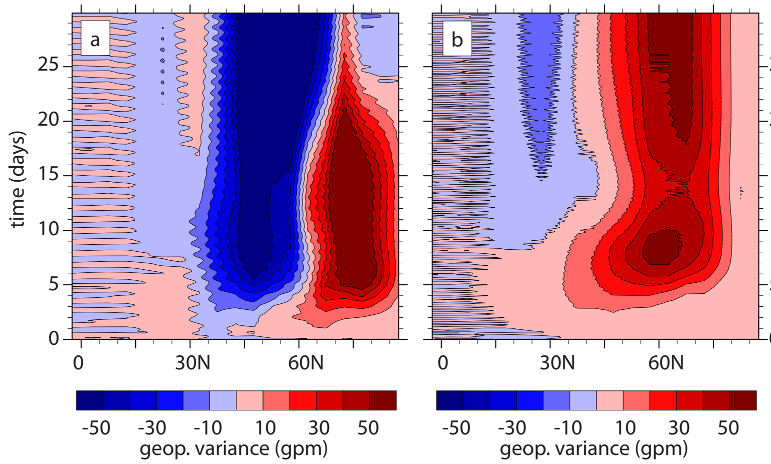

Petr Šácha 18.10.16 10:44
Deleted:

Petr Šácha 11.10.16 15:13

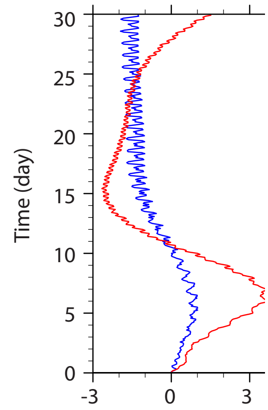

Deleted:

Unknown
Formatted: Font:Not Bold, Font color: Auto

Petr Šácha 11.10.16 15:14
Deleted: Fig.5: Time evolution of a sum of all harmonics' amplitude difference with respect to the reference run (a) and time evolution of the wave-1 amplitude difference (b) as given by the FT of geopotential at approximately 35km log pressure height for Box0.1 simulation minus FT amplitudes from Ref simulation at selected latitudes: 62.5°N (red) and 32.5°N (blue). Units are given in [gpm]. ... [92]

Unknown
Formatted: Font:Not Bold, Font color: Auto

Petr Šácha 11.10.16 15:14
Deleted: 6

Petr Šácha 13.10.16 14:24
Deleted: onthly m

Unknown
Formatted: Font:8 pt, Font color: Auto

Fig. 10: Time evolution of a wave-1 (a) and wave-3 (b) amplitude difference with respect to the reference run, as given by the FT of geopotential height at approximately 35km log pressure height for Box0.1 simulation. Units are given in [gpm].

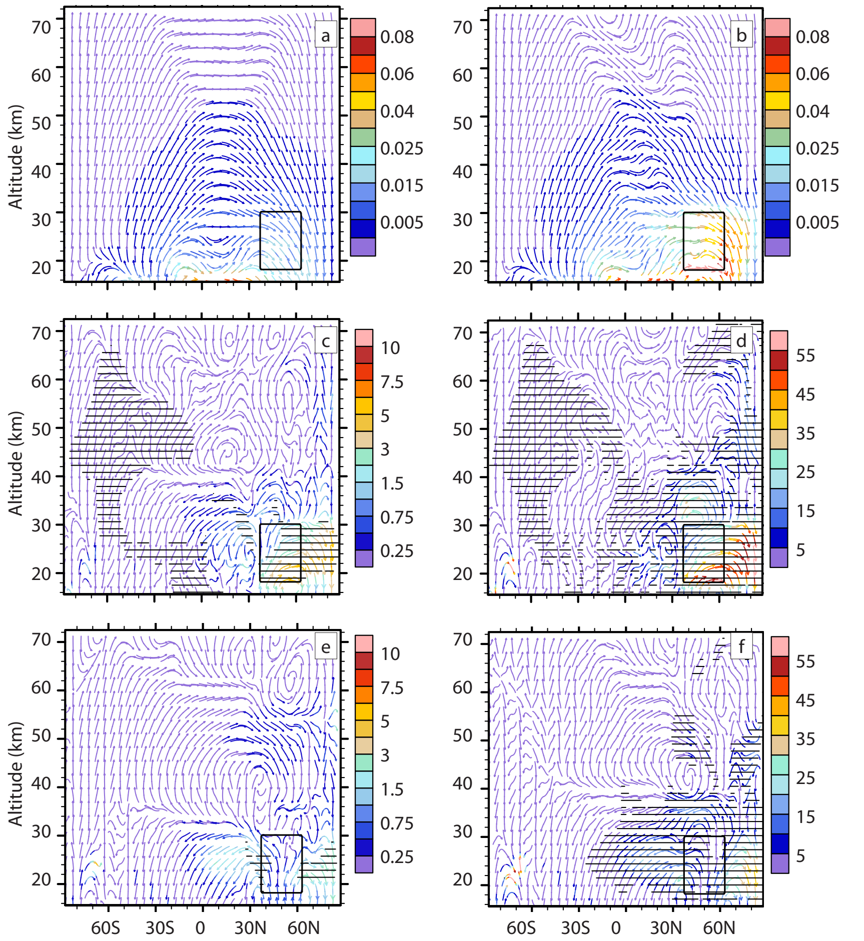

Fig. 11: Mean January zonal mean residual circulation (stream lines for illustration of direction only) and its mass flux (colors, in kgm^{2}s^{-2}) on the left (from top to bottom: Ref simulation (a), relative Box0.1- Ref simulation anomaly (c), relative Box0.1 - Zon0.1 simulation difference (e)) and on the right (from top to bottom: snapshot of the SSW box simulation at 5 days after the GWD injection (b), 10box - ref simulation relative anomaly (d), relative 10box - 10zon simulation difference (f)). Relative anomalies and differences are given in % of the reference or corresponding box simulation, respectively. The statistical significance of the mean residual circulation mass flux differences was computed by a t test and regions with *p* values < 0.05 are dashed.

Unknown
Formatted: Font:Not Bold, Font color: Auto

Petr Šácha 13.10.16 14:12

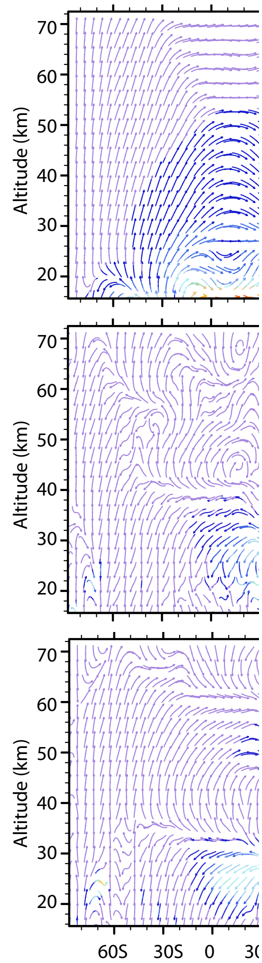

Deleted:

Unknown
Formatted: Font:Not Bold, Font color: Auto

Petr Šácha 13.10.16 14:12
Deleted: 7… Mean January zonal ... [93]

Petr Šácha 13.10.16 14:12

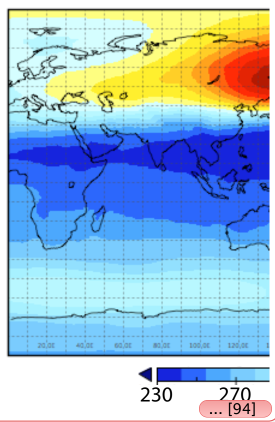

Deleted: ... [94]

Unknown
Formatted: Font:Not Bold, Italic, Font color: Auto

Unknown
Formatted: Font:(Default) Times New Roman, 8 pt, Bold

Petr Šácha 13.10.16 14:12
Formatted ... [95]

Petr Šácha 17.10.16 14:31

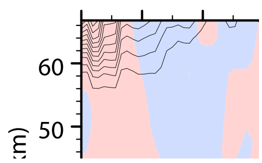

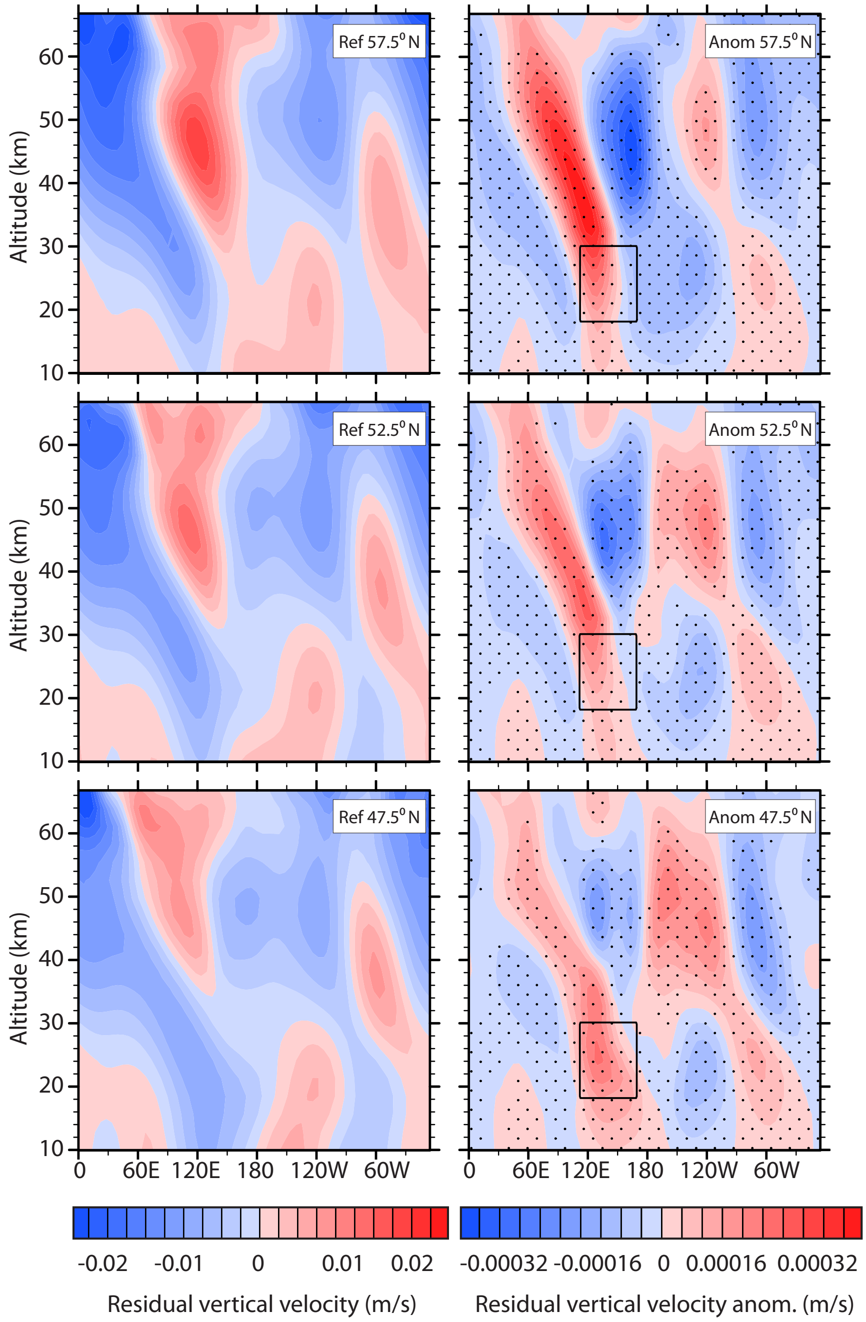

Fig. 12: Mean (7th to 30th day January longitudinal cross-sections of reference residual vertical velocity [ms-1] (on the left) and Box0.1 simulation anomalies (on the right) at selected latitudes. The contours illustrate the position of the artificial

Unknown
Formatted: Font:(Default) Times

Petr Šácha 17.10.16 14:31
Deleted: 0

Petr Šácha 17.10.16 14:34
Formatted: Superscript

Petr Šácha 17.10.16 14:34
Formatted: Superscript

Petr Šácha 17.10.16 14:33
Deleted:

Petr Šácha 17.10.16 14:33
Deleted: residual vertical velocity

Petr Šácha 17.10.16 14:33
Deleted: [ms-1]

Petr Šácha 17.10.16 14:33
Deleted: show gcu to

GWD. **The statistical significance of the mean anomalies was computed by a t test and regions with *p* values < 0.05 are stippled.**

Petr Šácha 17.10.16 14:33
Formatted: Justified